

4

Cardiovascular

Standard Imaging Methods for the Cardiovascular Region

A CT

Overview

1. Imaging and image reconstruction methods using ECG gating

The purpose of cardiac CT is often to evaluate the coronary arteries. Computed tomography angiography (CTA) and calcification scoring of the coronary arteries are performed for this purpose (Fig. 1). There are also various other applications of cardiac CT, such as myocardial wall motion evaluation (functional evaluation), tumor evaluation, and evaluation for atrial fibrillation ablation therapy.

Advancements in CT systems are important for the development of cardiac CT examination. The imaging method used varies depending on the type of equipment used, such as wide-detector (256 to 320 rows) MDCT, dual-source CT, and 64-row MDCT systems. This discussion focuses on cardiac CT using 64-row MDCT systems, the most widely available and basic type.

With the temporal resolution of CT, imaging of the heart while it is beating results in motion artifacts, which prevents accurate depiction of the structures of the heart, particularly the coronary arteries. In the mid-diastolic phase of the cardiac cycle (corresponding to 70% to 80% of the R-R interval), there is a period in which the heart moves slowly, and this brief period is used in coronary CTA. For example, if the heart rate is stable at approximately 60 beats per minute, 1 beat occurs per second, so the mid-diastolic phase lasts approximately 0.2 seconds. To accurately identify this brief period, ECG triggering or gating is required with cardiac CT. However, if the heart rate is high, imaging during systole (approximately 40% of the R-R interval) is often more appropriate than imaging during diastole. Because better image quality can generally be obtained with a low heart rate, it is important to control the heart rate using a beta-blocker (beta-1 selective). The beta-blocker is administered orally 1 hour before the test, by intravenous injection 5 minutes before the test, or both orally and intravenously. The optimal heart rate is below 60 beats per minute.

To obtain CT images, data for at least a half rotation plus the cone angle (half data) are required. In cardiac CT, reconstructing images from data for 1 rotation (full data) results in image quality improvement commensurate with the volume of data (image noise is reduced). However, cardiac motion greatly affects image quality, making it difficult to evaluate the coronary arteries. Consequently, image reconstruction in cardiac CT is performed based on half data (half reconstruction) to improve the temporal resolution. Split reconstruction (segment reconstruction and multisector reconstruction), wherein half data are obtained from the data for multiple heartbeats, is also used and may further increase the temporal resolution.

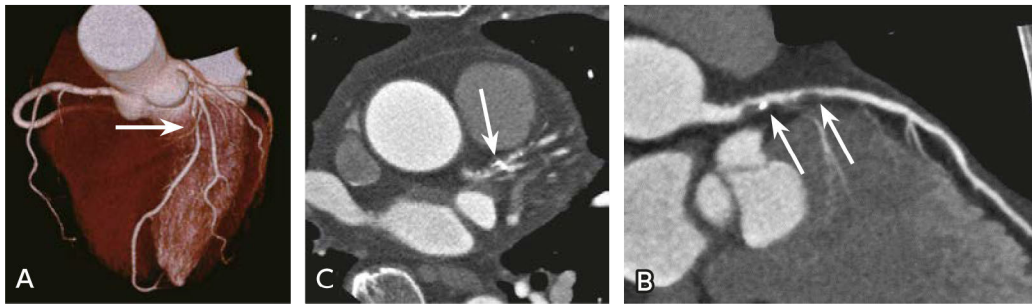


Figure 1. Coronary artery evaluation by cardiac CT

A: Volume rendering (VR) image; B: Original image, transverse; C: Curved MPR image

Severe stenosis resulting from a plaque with calcification is seen proximally in a coronary artery (left anterior descending artery).

There are two methods of ECG-gated CT. One is prospective ECG-gated scanning (ECG triggering), in which imaging is performed only during the ECG phase in which the pre-specified coronary artery motion is still (generally the mid-diastolic phase). The other method is retrospective ECG-gated reconstruction. With this method, data are acquired for all ECG phases, and image reconstruction is performed later by extracting images of interest for the cardiac standstill phase from the data. With 64-row MDCT, the extent that can be scanned at one time is limited to 3 to 4 cm, and cardiac CT images are generally acquired by retrospective ECG-gated reconstruction, which results in increased radiation exposure.

In recent years, wide-detector MDCT, which can allow high-speed rotation and cover the entire heart, and dual-source CT, which provides twice the temporal resolution, have also become widely used, and the use of prospective ECG-gated scanning has increased. These methods hold promise for reduced radiation exposure and high image quality.

2. Cardiac CT pretreatment, imaging, and contrast imaging protocols

Prospective ECG-gated scanning is generally performed for calcification scoring. Reconstruction is performed using a tube voltage of 120 kVp and a slice thickness of 2.5 to 3 mm. Tube current is determined according to body type to minimize radiation exposure, which should be approximately 1 to 2 mSv. Using dose modulation (Auto mA), image noise (SD) of 20 HU is commonly targeted.

With coronary CTA, breath-holding is practiced before the test. This is to prevent deviation from the imaging range, inhibit blurring caused by respiratory motion, and determine the changes in heart rate that occur during breath-holding. Physiologically, the heart rate often decreases during breath-holding. Therefore, depending on the circumstances, the dose of the intravenous beta-blocker used for coronary CTA can be reduced or its use avoided. Conversely, heart rate sometimes increases with breath-holding, and this information is useful for selecting the imaging and reconstruction methods. In addition, a nitrate preparation is recommended to dilate the coronary arteries and allow for more detailed coronary artery evaluation. However, because nitrate use generally increases the heart rate, it should be observed after a nitrate preparation is used.

For coronary CTA, an indwelling needle (20 G) is placed in the antecubital vein, and the contrast medium is injected using a dual-head automatic injector. The needle is attached to an extension tube and 3-way stopcock fitted with a syringe containing physiologic saline, and the apparatus can be flushed with contrast medium and physiologic saline. The 3-way stopcock is convenient for administering an injectable beta-blocker before the test. A high-concentration nonionic iodine contrast medium (350 to 370 mgI/mL) is used. Rapid injection is recommended, with an injection rate of 25 mgI/kg/s (fractional dose) considered standard.

Bolus tracking or test injection is used to determine the scan timing. With bolus tracking, a single-slice dynamic scan is performed before the actual scan, and the CT number in the blood vessel (aorta) is monitored in real time. When the target CT number is reached, the scan starts after a predefined time delay. The test injection method involves bolus injection of a small amount of contrast medium (10 to 20 mL) and measuring the contrast arrival time and time to peak contrast concentration from a single-slice dynamic scan to determine the timing of the actual scan.

Detailed discussion

1. Evaluating coronary artery lesions

A coronary artery calcification index (Agatston score) is calculated for the calcification score. The calcification score is useful for evaluating the risk associated with coronary artery lesions. For evaluating coronary lesions over time, maintaining consistent imaging conditions is important.

Coronary CTA provides particularly high sensitivity and negative predictive value for evaluating anatomical coronary artery stenosis. It plays a central role in current cardiovascular medicine as a noninvasive test for ischemic heart disease. It is useful for evaluating not only the severity of coronary artery stenosis, but also the characteristics of coronary artery plaques themselves (Fig. 2). It is also used for purposes such as evaluating coronary artery aneurysms associated with conditions such as Kawasaki disease, coronary artery malformation, and coronary artery bypass grafts (Fig. 3) and for evaluation after coronary stent placement (Fig. 4). However, coronary artery stent evaluations are affected by a number of factors, such as the stent material, coexisting calcification, and motion artifacts. Consequently, stents ≥ 3 mm in diameter that have been placed proximally in coronary arteries are indicated for stent evaluation at present.

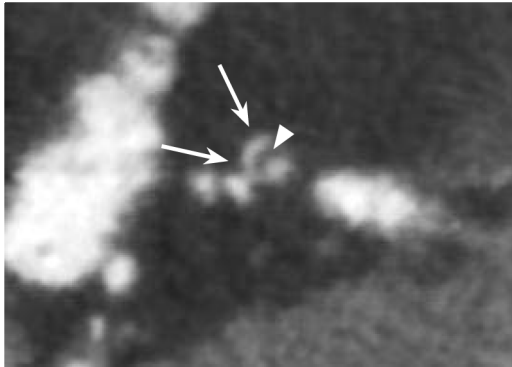


Figure 2. Evaluation of the characteristics of a coronary artery plaque (coronary CTA)

Short-axis MPR image of a coronary artery: A central necrotic core (hypodense component: \blacktriangleright) and enhancement of the plaque margin (\rightarrow) are seen. Referred to as a napkin-ring sign, it is a finding that indicates an unstable plaque.

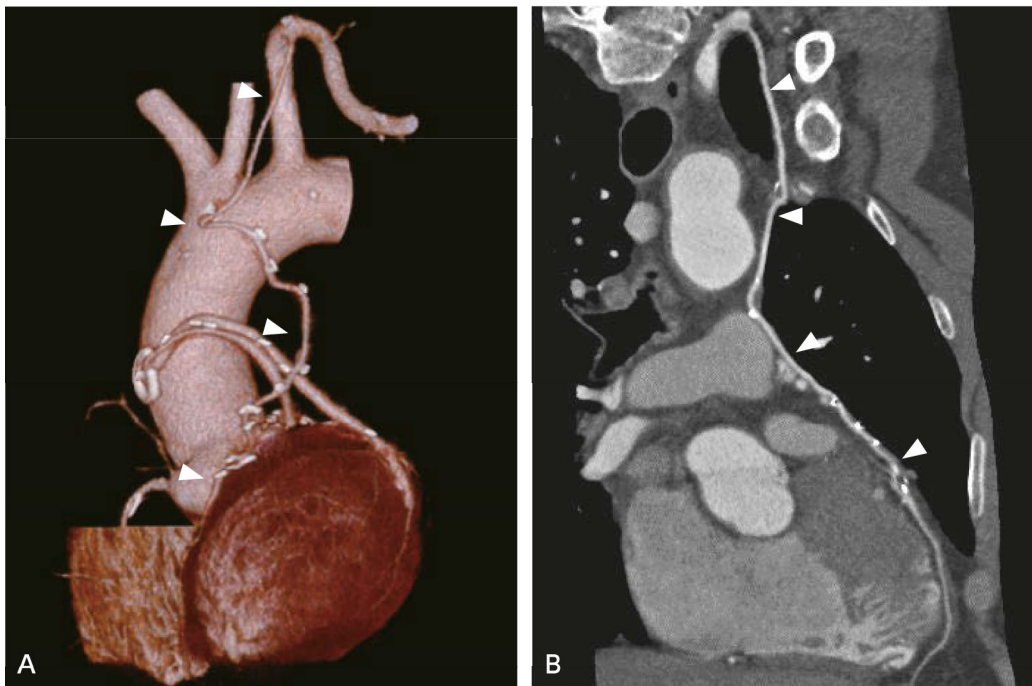


Figure 3. Evaluation of a graft after coronary artery bypass surgery (coronary CTA)

A: VR image, B: curved MPR image

Following coronary artery bypass surgery, the coronary artery (left anterior descending) is anastomosed to the left internal thoracic artery (\blacktriangleright). In addition, a diagonal branch and the circumflex artery are anastomosed, with the greater saphenous vein used as a graft.

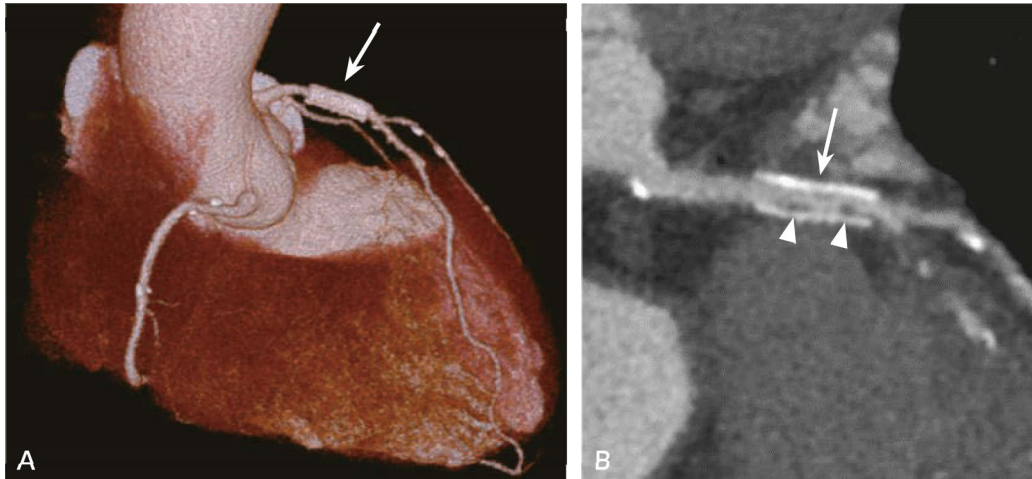


Figure 4. Evaluation after coronary stent placement (coronary CTA)

A: VR image, B: curved MPR image

A stent has been placed (→) proximally in the coronary artery (left anterior descending). Although the stent is patent, a hypodense component is seen in the lumen, suggestive of restenosis (▷).

2. Evaluating myocardial ischemia

The severity of anatomical coronary artery stenosis is not always consistent with that of a coronary lesion that induces hemodynamic myocardial ischemia. The methods used to evaluate functional stenosis by CT are myocardial CT perfusion imaging using pharmacological stress and fractional flow reserve CT (FFR-CT). Myocardial CT perfusion has disadvantages such as increased radiation exposure and a long test duration. However, an advantage is that it enables myocardial blood flow to be evaluated directly, and recent advances in CT systems and imaging technology have significantly reduced radiation exposure. FFR-CT is a simulation technique that estimates the myocardial fractional flow reserve (FFR) based on coronary CTA data.

3. Other cardiac evaluations

Coronary CT is also used to evaluate the location and size of the heart and blood vessels, fatty degeneration of the myocardium, cardiac tumors, valves, ventricle walls, the pericardium, and pericardial effusion accumulation. Appropriate indications for contrast-enhanced CT include evaluating intracardiac thrombus, cardiac tumors, pericardial and pericardiac lesions (inflammation and tumors), and congenital heart disease. With retrospective ECG-gated reconstruction, images can be acquired continuously in all ECG phases, enabling cardiac function, wall motion, and valve dynamics to be evaluated.

B MRI

Cardiac MRI

1. Overview

Cardiac MRI is an excellent noninvasive diagnostic modality for obtaining a wide variety of information, such as cardiac function, myocardial blood flow, myocardial viability, and coronary artery disease. Cardiac MRI enables all such essential information to be obtained with a single examination (so called one-stop shopping). However, the examination time is long and places a burden on the patient. Consequently, in actual practice, the appropriate imaging sequence is often selected according to the target disease or condition, and the purpose of the examination.^{8,9)}

① MR scanner and field strength considerations

Cardiac MRI always requires high temporal resolution to overcome the effects of heartbeats and respiratory motion. Use of a high-performance system is therefore necessary. Although systems with a magnetic field strength of 1.5T are most commonly used for cardiac MRI, examinations can also be performed with 3T systems. With 3T systems, sequences such as perfusion MRI and late gadolinium enhancement are beneficial for improving the signal-to-noise ratio (SNR). However, balanced steady-state free precession (bSSFP) imaging, a sequence used in cine MRI, is prone to problematic artifacts such as dark banding artifacts and flow artifacts, necessitating careful shimming.¹⁰⁾

② Specific surface coil and ECG-gating

A multi-element (typically ≥ 8 elements) surface coil for cardiac use is recommended. This allows improved temporal resolution using parallel imaging. ECG gating is typically used concurrently while acquiring images. Electrical signals should be collected in 3 dimensions with vector electrocardiography.

③ Reference cross-sections

In an actual examination, imaging is performed according to several reference cross-sections. As with other tomographic imaging methods such as echocardiography, the reference cross-sections make it easy to compare the results obtained using common cross-sections. Basic cross-sections include short-axis images of the left and right ventricles, perpendicular long-axis images of the left and right ventricles, horizontal long-axis images, 4-chamber long-axis images, 3-chamber long-axis images of the left ventricle, and long-axis images of the right ventricular outflow tract (RVOT).

2. Detailed discussion

① Cine imaging

Cine imaging can evaluate cardiac wall motion and function. It is currently the method that provides the most accurate and reproducible evaluations.¹¹⁾ The bSSFP sequence is used for cine imaging. With 3T systems, however, GRE is considered if artifacts become problematic.

When evaluating left ventricular structure and function, acquisition of left ventricle short-axis images from the mitral valve to the apex (Fig. 5A) is fundamental, and the images are used to measure left ventricular volume. In addition, horizontal long-axis images, 4-chamber long-axis images (Fig. 5B), perpendicular long-axis images of the left ventricle (Fig. 5C), and 3-chamber long-axis images of the left ventricle (Fig. 5D) are acquired and evaluated.

To evaluate right ventricular structure and function, right ventricle short-axis images are used. However, axial images can be used to measure right ventricular volume.¹⁰⁾ In addition, perpendicular long-axis images of the right ventricle and long-axis images of the RVOT are acquired and evaluated.

If evaluating interventricular interactions or performing conventional cine imaging is difficult (e.g., due to arrhythmias, breath-holding difficulty), real-time cine imaging can be used. However, it should be noted that the accuracy of quantitative evaluations may be lower due to the low temporal resolution.

It has recently become possible to quantitatively evaluate myocardial strain from conventional cine imaging images using the feature tracking method. This has been found to be useful for early diagnosis and outcome prediction in myocardial ischemia and many cardiomyopathies, and it is used as an optional technique.¹²⁾

② First pass perfusion

Myocardial perfusion imaging involves intravenous bolus injection of gadolinium contrast medium and evaluating myocardial blood flow based on first-pass hemodynamics. It is used to diagnose myocardial ischemia.¹³⁾ It has high detectability to diagnose ischemia and is excellent for diagnosing subendocardial ischemia and severe 3-vessel disease, which are difficult to diagnose with conventional SPECT.¹⁴⁾

The pulse sequences are typically saturation recovery (SR) imaging with bSSFP, GRE, or GRE-EPI hybrid read out. Left ventricle short-axis images (at least 3 slices per heartbeat) are acquired, with images acquired for every heartbeat. Coronary vasodilators such as adenosine, ATP, and dipyridamole are normally used in evaluating ischemia.

③ Late gadolinium enhancement (LGE)

With this technique, image acquisition is performed after gadolinium contrast medium is injected intravenously, when the concentration of contrast in the blood and extracellular fluid reaches equilibrium. The reduction in myocardial cell volume and myocardial fibrosis (increased extracellular fluid fraction) are then evaluated.¹⁵⁾ LGE MRI makes it possible to visualize myocardial lesions with high reproducibility. It has been shown to be useful for differential diagnosis and prognosis assessment in a variety of diseases, such as cardiomyopathy, myocarditis, and ischemic heart disease, in particular.¹⁶⁾

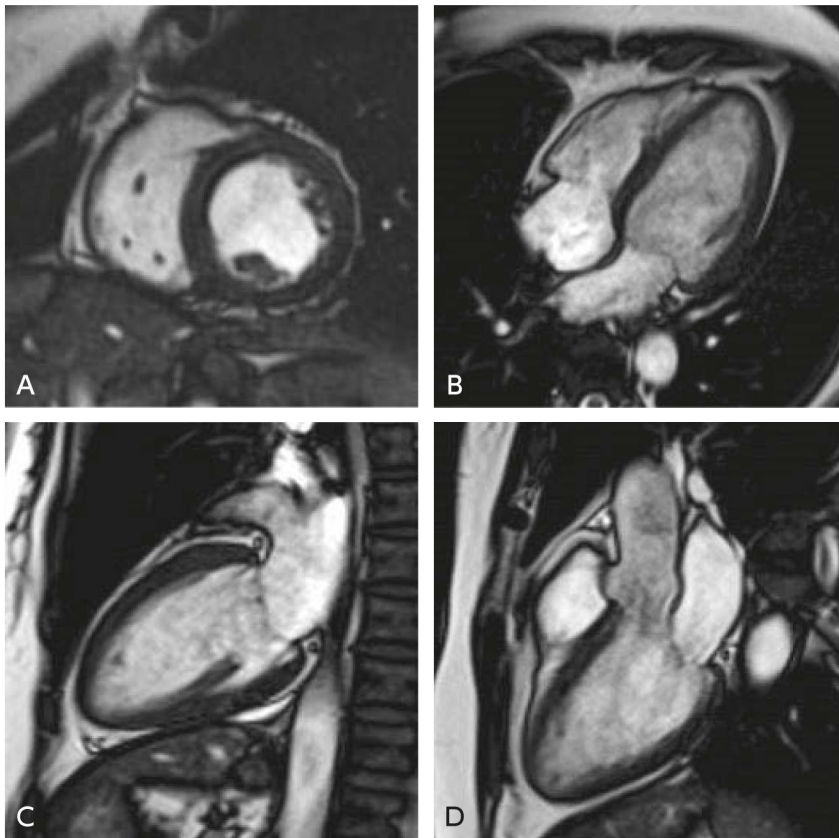


Figure 5. Cine imaging (bSSFP sequence) in a healthy individual

A: Left ventricle short-axis image, B: 4-chamber long-axis image, C: Perpendicular long-axis images of the left ventricle, D: 3-chamber long-axis image of the left ventricle

When adequate breath-holding is possible, the pulse sequences are a 2D IR GRE, 2D IR bSSFP, phase-sensitive IR (PSIR), or 3D sequence.¹⁰ If the patient has an arrhythmia or difficulty with breath-holding, a single-shot bSSFP sequence is used.

Specifying an appropriate time of inversion (TI) nulls the signal intensity of normal myocardium, enabling a lesion to be visualized as a distinct hyperintensity (Fig. 6).

LGE is performed after waiting for at least 10 minutes after gadolinium contrast medium injection. However, if the dose of contrast medium is low, LGE is performed less than 10 minutes after injection; otherwise, adequate lesion visualization cannot be obtained.

④ Coronary MRA

Coronary MRA is used mainly to evaluate coronary artery morphology in the case of coronary artery malformation or coronary artery aneurysms associated with Kawasaki disease, or when a contrast medium cannot be used.⁸ It has the advantages that it can be performed without the use of a contrast medium or radiation exposure. However, its spatial resolution does not equal that of X-ray coronary angiography or coronary CTA.

The 3D sequence, which images the entire heart at once, is commonly used. Imaging is performed under free-breathing conditions in combination with respiratory gating (navigator echo method), which is highly accurate.^{17, 18)} If respiratory gating cannot be used, or poor imaging quality is obtained, breath-hold imaging is also considered. Blood vessel visualization can also be improved using a gadolinium contrast medium.

⑤ Blood flow measurement

MRI is used to evaluate blood flow status and intracardiac shunts in valvular heart disease, aortic disease, and congenital heart disease. In coronary artery disease, it is also used to evaluate blood flow in coronary arteries and bypass grafts, and to determine coronary flow reserve by measuring blood flow in the coronary sinus.⁸⁾

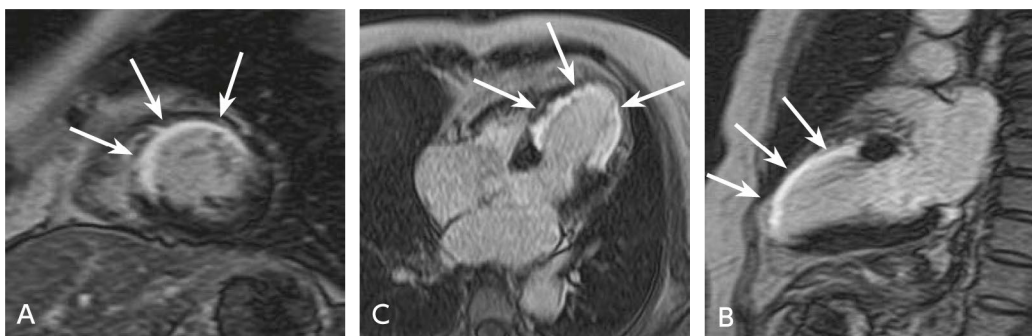


Figure 6. Late gadolinium enhancement (3D IR GRE sequence) of myocardial infarction (old infarct)

A: Left ventricle short-axis image, B: 4-chamber long-axis image, C: Perpendicular long-axis image of the left ventricle
Contrast enhancement is seen in an infarct centered on the region from the anterior wall of the left ventricle to the interventricular septum (→).

The sequence most commonly used to measure blood flow is phase contrast cine GRE with the flow encoding set perpendicular to the imaging plane. With phase contrast MRI, phase contrast images are obtained in addition to normal magnitude images, and the signal of phase contrast images is proportional to blood flow velocity.

Four-dimensional flow MRI, which can perform 3D measurements in multiple planes and enable serial observations, has become widely available in recent years, and its use is considered whenever possible.¹⁹⁾

⑥ Advanced tissue characterization

Methods used to evaluate myocardial characteristics include T1 mapping, T2 mapping, T2-weighted imaging, and T2* mapping.^{10,20)} This area is a rapidly developing field, and the imaging methods that can be used vary between manufacturers and systems. It should be noted that the normal values vary depending on the facility, system, and sequence used.²⁰⁾

MRI and MRA of the aorta and peripheral vasculature

1. Overview

The main purpose of MRI and MRA in the aorta and peripheral vasculature is to evaluate lumen diameter and hemodynamics in combination with vessel wall assessment.²¹⁾ The MRA is categorized as contrast-enhanced MRA, which is performed with intravenous injection of gadolinium contrast medium, and non-contrast-enhanced MRA, which is performed without the contrast medium.²²⁾ Contrast-enhanced MRA is little affected by blood flow velocity, enabling highly reproducible images to be obtained in a short time. However, it has been shown to be associated with a risk of nephrogenic systemic fibrosis (NSF) in patients with severe nephropathy, and its use has declined in recent years with advances in non-contrast-enhanced MRA imaging methods. Cine MRI and methods that involve the intravenous bolus injection of contrast medium are used to evaluate hemodynamics. Imaging methods such as SE are used to evaluate the vessel walls. Recently, however, the method called plaque imaging, the purpose of which is to perform qualitative plaque assessment, has been introduced into practical use, particularly for evaluating the carotid arteries.²³⁾

2. Detailed discussion

① Contrast-enhanced MRA

Contrast-enhanced MRA uses the T1 attenuation effect of blood to visualize the vessel lumen as a hyperintensity with gadolinium contrast medium. A fast 3D GRE sequence is typically used. Its strengths are that it is little affected by blood flow velocity or direction or by turbulence, and it enables extensive imaging in a relatively short time.²⁴⁾ Following an intravenous bolus of contrast medium, hemodynamics is observed by continuously collecting multiphase data using imaging techniques with high temporal resolution.

② Non-contrast-enhanced MRA

Typical imaging methods are time-of-flight (TOF) sequences, which use the blood influx effect, and phase contrast (PC) sequences, which reflect the spin phase contrast of blood flow. However, PC sequences are used only for the evaluation of function that reflects phase information. TOF sequences comprise 3D TOF and 2D TOF sequences. The former are used mainly for arteries with high blood flow velocity that require high spatial resolution, such as the craniocervical arteries. The latter are appropriate for blood flow visualization in vessels with low flow rates, such as the arteries and veins of the extremities. Recently, ECG-gated 3D fast SE sequences (Fig. 7) and bSSFP sequences are also being used (Fig. 8A). ECG-gated 3D fast SE sequences use the differences in the blood flow patterns in systole and diastole determined using ECG gating. The bSSFP sequences reflect T2/T1 contrast and visualize the blood as hyperintensity.²⁵⁾

③ MRI

SE and fast SE sequences are commonly used. Blood flow in the lumen and the characteristics of the vessel wall can be clearly visualized without using a contrast medium. The imaging time is generally long,

and the images are susceptible to respiratory artifacts and signals from turbulence and slow blood flow. To suppress blood flow signals and prevent artifacts, the black blood sequence, which uses a double IR pulse, is used (Fig. 8B).²⁶⁾

Numerous sequences have been proposed for plaque imaging, and it has not been standardized. In essence, however, blood flow signals are suppressed using double saturation pulses or a double IR pulse, and features such as intraplaque hemorrhage and the fibrous components of plaques are evaluated.²³⁾



Figure 7. Non-contrast-enhanced MRA from the pelvis to femoral region in arteriosclerosis obliterans (ECG-gated 3D fast SE sequence)

Extended tortuosity is seen in the iliac artery. However, no apparent occlusion or significant stenosis is seen in the visualized extent.

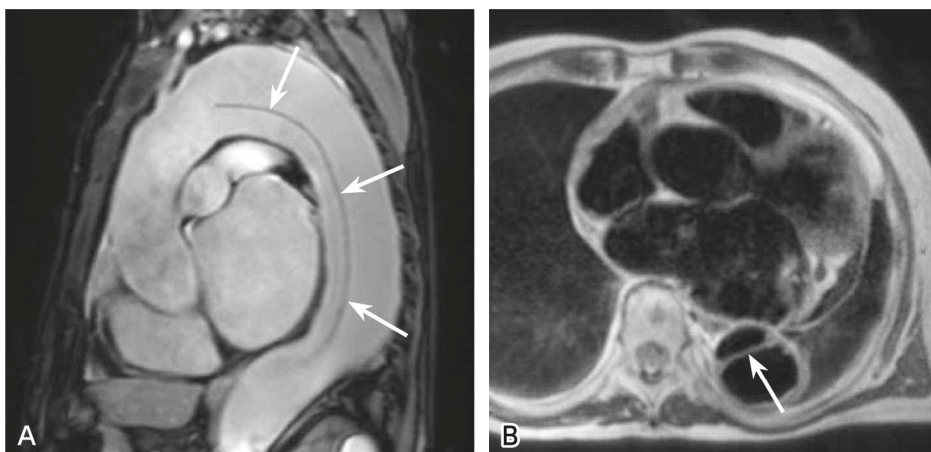


Figure 8. Non-contrast-enhanced MRI (MRA) of a communicating aortic dissection

A: bSSFP sequence, sagittal image; B: Black blood sequence, transverse image

The flap is clearly visualized (→).

C Angiography

Overview

With the development of noninvasive imaging modalities such as CT, MRI, and ultrasonography, angiography is being used less frequently as definitive diagnostic imaging in the cardiovascular region. Although cardiac catheterization (coronary angiography) remains a gold standard for examining coronary artery disease, the role of angiography is shifting to that of a therapeutic adjunct for the great vessels and peripheral vessels. However, angiography has some advantages not provided by other modalities, and it is therefore important to understand and take advantage of its features.

1. Features of angiography

Vascular structure and territory can be imaged in detail with angiography by selectively administering contrast medium to the vessel of interest. Imaging was initially performed using X-ray film in single shots. In addition to real-time fluoroscopy, continuous imaging by automatic film exchange became possible. Subsequently, the manual subtraction method was proposed, in which two X-ray films were used to perform imaging before and after contrast medium administration, and this particularly came to be used for cranial angiography.

Since digital image data became available, serial imaging and semi-automatic subtraction methods have become widely used. In particular, the subtraction technique, which is called digital subtraction angiography (DSA), is commonly used in thoracic and abdominal angiography.

Spatial and temporal resolutions are generally higher than with other imaging modalities. However, this procedure is highly invasive because selective imaging requires the use of a catheter. Imaging can also be performed with intravenous contrast agents, but resolution is reduced in areas of low contrast medium concentration. Consequently, selective imaging with transarterial contrast medium injection is normally performed.

Imaging frame rates of up to 15 to 30 fps can be selected, although this depends on the system. Taking into account radiation exposure, imaging with the minimum frame rate required for the pathology is recommended.

The direction and velocity of blood flow can be qualitatively evaluated by observing angiograms in video form. However, areas not filled with contrast medium are difficult to evaluate.

2. Classification according to imaging method

In recent systems, digitization of the image takes place, and the signal detectors have shifted from acquisition with a charge-coupled device (CCD) via an image intensifier to flat-panel X-ray sensors (Fig. 9).

① Digital angiography (DA, Fig. 10)

Digital angiography images are provided as projection images similar to those of X-ray fluoroscopy. Because the contrast of X-ray density is projected, not only the contrast medium, but also high-density structures such as bone and low-density structures such as the lungs are visualized simultaneously. For this reason, analog imaging suffers from image quality deterioration due to halation and insufficient radiation dose, but digitization has improved these problems and reduced radiation dose. A typical example of the use of DA in the cardiovascular region is coronary angiography. DA enables imaging to be performed while moving the table to follow the flow of contrast medium.

The imaging conditions vary depending on the patient's body type and location of imaging and the purpose of the test. For non-pediatric patients, frame rates of ≤ 15 fps are commonly used.

② Digital subtraction angiography (DSA) (Fig. 11)

DSA uses the difference between images before and after administration of contrast medium to selectively display contrast-enhanced areas²⁷⁾. The signal intensity of areas not filled with contrast is nulled by subtraction processing, and these areas are not visualized. Therefore, even in areas where the background X-ray transmittance is not uniform, which are difficult to observe with normal imaging, lesions can be easily observed by improving the contrast between lesions and healthy areas. Furthermore, DSA can visualize even slight changes in contrast, making it suitable for detailed diagnosis. However, object motion is rendered as artifacts, so the heartbeat, gastrointestinal peristalsis, and poor breath-holding can be problematic.

As with DA, the imaging conditions used depend on the patient and the purpose of the imaging procedure. However, radiation exposure tends to be higher than with DA, so selection of appropriate imaging conditions is important.

(1) DSA using a fixed table

A wide field of view is selected to image large blood vessels, and a narrow field of view is selected to magnify organs and lesions for selective angiography. Because the size of the field of view that can be selected depends on the system, it is important to select a system suitable for the purpose of the imaging procedure.



Figure 9. Flat-panel vascular imaging system

Pictured is a biplane system that uses flat-panel detectors. The small volume of the detectors somewhat reduces the limitations on aspects such as imaging angles. However, the imaging angles that can be used vary depending on the size of the panels.



Figure 10. Digital angiography (DA)

Contrast-enhanced arteries and part of the femur are seen. The image is comparable to images obtained by normal fluoroscopic imaging.

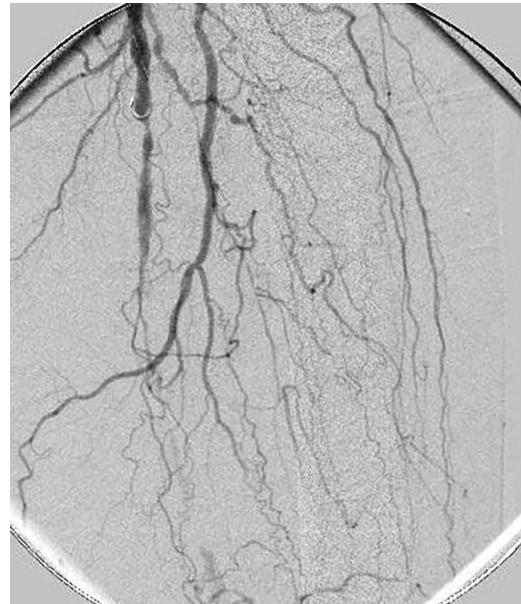


Figure 11. Digital subtraction angiography (DSA)

A subtraction image of the same location shown in Fig. 10. The background is visualized homogeneously as a result of subtraction processing, so that only the contrast-enhanced arteries are observed, enabling details to be evaluated.

(2) DSA using a moving table

Used mainly to image a long extent such as the arteries of the lower extremities, this method is called stepping DSA^{28, 29)} or bolus chase DSA.³⁰⁾ Because a long area is imaged with a single administration of contrast medium, the contrast medium dose and radiation exposure can be reduced. However, it should be noted that this imaging method is not available on all systems.

(3) Rotational angiography³¹⁻³³⁾

This method enables the structure of vessels to be determined in 3 dimensions by rotating the arm of the angiography system around the subject, with the table fixed, and performing continuous imaging from multiple angles. This is also called cone-beam CT (CBCT). Observations can be carried from unlimited projection angles using reconstructed images. Examples of such use include examining the neck of an aneurysm and visualization of overlapping branch vessels. This method is commonly used for cerebral angiography. Recently, however, this method has been applied to abdominal angiography, such as hepatic arteriography, to provide information on three-dimensional vascular anatomy during interventional radiology (IVR) to assess feeding vessels of target lesions. Subtraction processing is also often used to improve observation precision.

3. Applications of angiography for the heart and great vessels

Due to its invasiveness, angiography is of limited use and is rarely used for simple diagnostic purposes. Although angiography is the gold standard for diagnosing coronary artery disease, it is advisable to carefully consider the risk of disease before choosing any imaging procedure. In recent years, screening use of coronary CT prior to percutaneous coronary intervention (PCI) has become common, and as a result, angiography tends to be used for treatment rather than diagnosis.

Examining the great vessels does not require as much spatial resolution as coronary artery imaging, and the role of angiography is limited, because information about vessel walls, plaques, and mural thrombi is important for understanding pathophysiology and cannot be assessed by angiography. However, depending on the status of the patient and disease, evaluation by angiography, which provides excellent selective visualization of vessels and spatial resolution, is required in cases such as when endovascular therapy is immediately implemented.

4. Typical diseases for which angiography is performed

① Aortic aneurysm

Because noninvasive evaluation by CT,³⁴⁾ ultrasonography,³⁵⁾ and MRI is widely performed, the use of angiography is limited for purposes such as performing an evaluation just before stent-graft insertion.

② Aortic dissection

In the acute phase, there is a risk that catheter insertion or rapid injection of contrast medium will exacerbate the condition. Consequently, angiography is currently not used for aortic dissection, and initial diagnosis is commonly performed by ultrasonography or CT.^{36, 37)} The indications for angiography are considered to be limited to uses such as stent-graft insertion to occlude entry or to dilate the true lumen and branch stenoses.

③ Vasculitis

Vasculitis-related disorders such as Takayasu's arteritis and inflammatory aortic aneurysm are diagnosed mainly by CT and MRI.³⁸⁻⁴²⁾ Determining the condition of the vessel wall is particularly important in vasculitis, and angiography is unsuitable for initial diagnosis. Moreover, fragility of the vessel wall is common in vasculitis-related conditions such as vascular Behçet's disease, and the invasiveness of catheter insertion risks exacerbation. Consequently, the use of angiography must be considered carefully.

④ Pulmonary thromboembolism

As is the case with other disorders, pulmonary thromboembolism is diagnosed by means such as contrast-enhanced CT,⁴³⁾ and angiography is rarely used for its diagnosis. However, it is used for purposes such as preoperative evaluation for transcatheter thrombus aspiration and thrombolysis and in chronic pulmonary thromboembolism.

⑤ Arteriosclerosis obliterans

Angiography is performed for this condition when surgery or endovascular therapy is planned. As in other vascular pathologies, the actual diagnosis of the disease is commonly performed by CT or MRI. However, if the artery wall is severely calcified, or lesions are severe, it is important to determine the patency of collaterals and vessels below the arteries of the lower extremities, and angiography may therefore be selected.

⑥ Acute arterial occlusion

Although the opportunities to use ultrasonography and CT for acute arterial occlusion are increasing, angiography is still selected to definitively determine the location of the embolism, the extent of the occlusion, and the patency of peripheral vessels. Angiography may also be performed intraoperatively.

Depending on the healthcare facility's approach and the patient's condition, transcatheter thrombus aspiration or thrombolysis may be performed, and angiography is concurrently used in such cases.

⑦ Thromboangiitis obliterans (Buerger's disease)

The estimated age of onset is in the 30s and 40s, and the condition is common in male smokers.⁴⁴⁾ However, the bulk of the patients are aged 45 to 55 years, suggesting that the age of onset is increasing. The collaterals that develop in association with peripheral vascular occlusion have a characteristic tortuous appearance. Corkscrew-shaped collaterals develop,^{45, 46)} and characteristic findings such as standing waves⁴⁵⁾ are seen on angiography, making it of high diagnostic value. However, these findings can also often be observed on CT and MRI, and the use of angiography for diagnostic purposes is waning.

D Nuclear cardiology

Overview

The introduction of new image reconstruction methods with spatial resolution recovery and noise suppression and dedicated cardiac gamma cameras with special semiconductor detectors (CZT) has made it possible to reduce patient radiation exposure (Table 1) during Nuclear cardiology imaging.^{47, 48)} The following practices are recommended to reduce radiation exposure during myocardial perfusion SPECT imaging (SPECT-MPI): low-dose ^{99m}Tc imaging, stress-only imaging with a ^{99m}Tc tracer, calculating the dose based on the body mass index (BMI), reducing artifacts by attenuation correction, and avoiding the use of ²⁰¹Tl alone and dual-isotope imaging with both ^{99m}Tc and ²⁰¹Tl.^{49, 50)} However, a weakness of ^{99m}Tc agents is that they accumulate at higher levels in the digestive tract than ²⁰¹Tl.⁵⁰⁾ Using a cardiac-dedicated CZT gamma camera and the latest reconstruction methods, imaging can also be performed with a ²⁰¹Tl agent at a low dose.⁴⁷⁾ Consequently, the radionuclide to be used should be selected by taking into account both the characteristics of the 2 radionuclides and the equipment at each facility. As the development of ¹⁸F myocardial perfusion agents progresses, PET myocardial perfusion imaging (PET-MPI) is also expected to become an option in the future.^{49, 50)}

Table 1. Low-dose testing with the use of new image reconstruction methods or new cardiac-dedicated gamma cameras

Protocol	1st Acquisition			2nd Acquisition			Total Effective Dose (mSv)	Stress Only (effective dose: mSv)
	Stress/Rest	Dose Administered, MBq (mCi)	Effective Dose (mSv)	Stress/Rest	Dose Administered, MBq (mCi)	Effective Dose (mSv)		
^{99m}Tc 1-Day Protocol								
Stress/Rest	Stress	148–222 (4–6)	1.0–1.5	Rest	444–666 (12–18)	3.5–5.2	4.6–6.7	1.0–1.5
Rest/Stress	Rest	148–222 (4–6)	1.2–1.7	Stress	444–666 (12–18)	3.0–4.5	4.2–6.3	n/a
^{99m}Tc 2-Day Protocol								
Stress/Rest	Stress	148–222 (4–6)	1.0–1.5	Rest	148–222 (4–6)	1.2–1.7	2.2–3.3	1.0–1.5
Rest/Stress	Rest	148–222 (4–6)	1.2–1.7	Stress	148–222 (4–6)	1.0–1.5	2.2–3.3	n/a
²⁰¹Tl								
Stress/Redistribution	Stress	48.1–66.6 (1.3–1.8)	5.7–7.9	n/a	n/a	n/a	5.7–7.9	n/a
Dual radionuclides (²⁰¹Tl/^{99m}Tc)								
²⁰¹ Tl rest/ ^{99m} Tc stress	Rest	48.1–66.6 (1.3–1.8)	5.7–7.9	Stress	148–222 (4–6)	1.0–1.5	6.7–9.4	n/a
²⁰¹ Tl stress/ ^{99m} Tc rest	Stress	48.1–66.6 (1.3–1.8)	5.7–7.9	Rest	148–222 (4–6)	1.2–1.7	6.9–9.6	5.7–7.9

n/a: not applicable

Effective dose of ^{99m}Tc: Mean dose for ^{99m}Tc-MIBI and ^{99m}Tc-tetrofosmin. The tissue weighting factors (weightings) of ICRP publication 103 were used to calculate the effective doses.

Aside from myocardial perfusion imaging, ¹²³I-MIBG is used for prognosis prediction in heart failure. It is also used to diagnose Parkinson's disease and Lewy body dementia.^{50, 51)} Recently, bone scintigraphy agents (^{99m}Tc-pyrophosphate in Japan) have been used to diagnose cardiac amyloidosis,⁵²⁾ and ¹⁸F-FDG has been used to diagnose cardiac sarcoidosis.⁵³⁾ It is recommended that nuclear cardiology imaging be optimized for the individual patient with respect to aspects such as indications and dose.⁴⁸⁾ The following discussion focuses on standard imaging methods for nuclear cardiology testing.

Detailed discussion

1. Myocardial perfusion SPECT imaging methods (SPECT-MPI)

① Features of myocardial perfusion agents

The agent ²⁰¹Tl is a monovalent cation that, like potassium, is taken up by the myocardium by active transport and has a high first-pass extraction fraction (85%). A feature of ²⁰¹Tl is that its washout from the myocardium begins 10 to 15 minutes after administration.⁴⁷⁾ Its washout over time is slower in ischemic myocardium than in normal or infarcted myocardium. Consequently, in delayed images, redistribution is

seen in ischemic myocardium, but not in infarcted myocardium (Fig. 12). The ^{99m}Tc agents [^{99m}Tc -methoxyisobutylisonitrile (MIBI) and ^{99m}Tc -tetrofosmin] are fat-soluble and passively taken up by the myocardium in proportion to blood flow. Within the myocardium, they are voltage-dependently sequestered in the mitochondrial inner membrane as monovalent cations.⁴⁷⁾ However, their first-pass extraction fractions are lower than of ^{201}Tl , and they are not washed out over time.⁴⁷⁾ Consequently, to distinguish ischemic from infarcted myocardium, they must be administered twice, once under stress and once at rest.

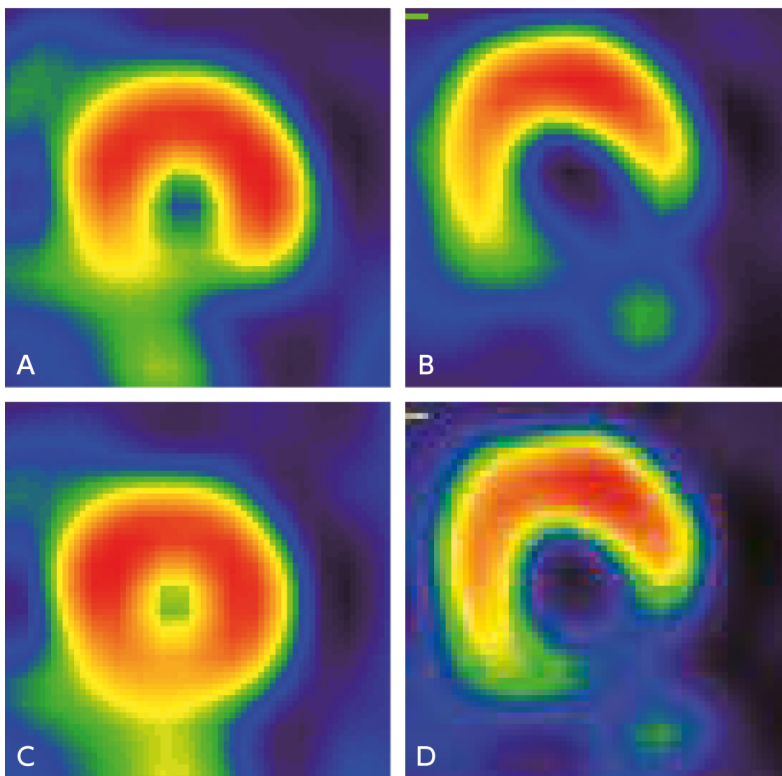


Figure 12. Ischemic and infarcted myocardium (^{201}Tl stress myocardial perfusion SPECT)

A, B: Stress image; C, D: Delayed image; A, C: Ischemic myocardium; B, D: Infarcted myocardium

In ischemic myocardium, decreased blood flow is seen in the inferior wall in the stress image (A), and redistribution is seen in the inferior wall in the delayed image (C). In infarcted myocardium, a perfusion defect is seen from the inferior wall to part of the lateral wall in the stress image (B), but redistribution is not seen in the delayed image (D).

② Stress methods

Exercise stress is applied in multiple steps using a treadmill or bicycle ergometer. Because diagnostic performance decreases if the exercise load is inadequate, the target workload is 85% of the predicted maximum heart rate. The myocardial perfusion agent is administered during maximum stress, and the stress is discontinued 60 to 90 seconds after administration. Adenosine is generally used for pharmacological stress. Adenosine is administered continuously over 6 minutes at a rate of 0.12 mg/kg/min, and the myocardial perfusion agent is administered 3 minutes after the start of adenosine administration. Because

caffeine is an adenosine antagonist, its ingestion is prohibited for 12 hours before adenosine administration. Regadenoson, a newly developed selective adenosine A_{2A} receptor agonist, enables stress to be applied with a single intravenous injection.⁴⁷⁾ However, it has not been introduced in Japan.

③ Myocardial perfusion SPECT imaging

Table 2 summarizes the main recommendations of level IIa or higher for nuclear cardiology imaging provided in the JCS 2018 Guideline on Diagnosis of Chronic Coronary Heart Diseases,⁵⁰⁾ along with the MINDS recommendation grades.

Because stress electrocardiography is performed first, the guidelines indicate that a good indication for myocardial perfusion SPECT is when ECG evaluation is difficult or there is an abnormal finding on ECG. It is considered useful for diagnosis when the pre-test probability is moderate or greater with typical chest pain. However, coronary CT angiography is also currently recommended if CT can be performed. Whether to perform coronary CT angiography or nuclear cardiology imaging first for diagnosis is not always clear. The most recent guidelines of the European Society of Cardiology (ESC) recommend that a pretest ECG be used to evaluate the risk of coronary artery disease rather than for diagnosis and that coronary CT angiography, with its high negative likelihood ratio, be used for exclusion of coronary artery disease in groups at low risk. In groups at high risk of coronary artery disease, the guideline recommends that nuclear cardiology imaging be used for definitive diagnosis because of its high positive likelihood ratio.⁵⁴⁾ In addition, nuclear cardiology imaging has been shown to be useful for prognosis prediction in patients at moderate risk of coronary artery disease, although this is not indicated in the table.⁵⁴⁾

Table 2. Recommendation classes and MINDS recommendation grades for the main nuclear cardiology imaging

Item	Recommendation Class	Recommendation Grade
Myocardial perfusion SPECT (²⁰¹Tl, ^{99m}Tc-MIBI, ^{99m}Tc-tetrofosmin)		
Patients for whom ECG evaluation is difficult (limited to pharmacological stress in conditions such as complete left bundle branch block and ventricular pacing)	I	B
Abnormal stress ECG	I	B
Moderate or higher pre-test probability and typical anginal pain	I	B
Presence of residual ischemia from known coronary artery disease and regional diagnosis to be performed	I	B
For regional diagnosis of myocardial infarction	I	B
To determine whether coronary revascularization indicated	I	B
Patient with moderate or higher pre-test probability or atypical chest pain and coronary artery calcium score (CACS) ≥ 400		
To perform functional stenosis assessment of moderately severe (40% to 75%) stenotic lesion	IIa	C1
To evaluate treatment efficacy	IIa	C1
When performing pharmacological stress test because exercise stress cannot be used, although pre-test probability is moderate or higher	IIa	C1
Cardiac sympathetic innervation (¹²³I-MIBG)		
Prognostic assessment of ischemic heart failure	IIa	B
Myocardial fatty acid metabolism (¹²³I-beta-methyl-p-iodophenyl-pentadecanoic acid, BMIPP)		
Cardiomyopathy ischemia diagnosis and prognostic assessment/risk stratification	I	B
Myocardial ischemia diagnosis, prognostic assessment/risk stratification, vasospastic angina diagnosis	IIa	B
Myocardial glucose metabolism (¹⁸F-FDG, myocardial viability evaluation)		
In patients with coronary artery disease and severe left ventricular dysfunction, to evaluate prognosis and the extent of myocardium that may recover with coronary revascularization or for heart transplant.	I	B
Performed in patients with myocardium with a fixed perfusion defect of moderate or greater severity or patients with an inconclusive diagnosis based on other tests.	I	B
Myocardial perfusion PET (¹⁵N-ammonia)		
Diagnosing coronary artery disease in patients with a moderate to high pre-test probability	I	A
Risk stratification and prognostic assessment based on ischemia and amount of infarcted myocardium	I	A
Risk stratification and prognostic assessment based on quantitative analysis of myocardial perfusion	I	A
Risk stratification and prognostic assessment based on analysis of left ventricular function using ECG gating	IIa	B
Detecting left main disease and severe multivessel disease by quantitative analysis of myocardial perfusion	IIa	B

Recommendation classes

I: There is evidence or a broad consensus that the procedure or treatment is effective and useful.

IIa: Based on the evidence and opinions, it is highly likely that the procedure or treatment is effective and useful.

MINDS recommendation grades

A: Procedure strongly recommended, since there is strong scientific basis for performing it.

B: Procedure recommended, since there is scientific basis for performing it.

C1: Procedure recommended, although there is no scientific basis for performing it.

2. Imaging methods for myocardial perfusion PET

The myocardial perfusion agents for PET include ^{82}Rb , ^{15}O -water, and ^{13}N -ammonia (NH_3). In Japan, only ^{13}N -ammonia is covered by national health insurance.⁵⁰⁾ ^{13}N -ammonia is taken up by the myocardium by passive diffusion or as monovalent ammonia ions by active transport via the sodium-potassium pump. The ^{13}N -ammonia that is taken up by the myocardium is incorporated into the amino acid pool as ^{13}N -glutamine, where it accumulates.^{50, 55)} ^{13}N has a relatively long half-life of 10 minutes, and its short positron range enables visual assessments to be performed with good image quality. Moreover, it has a good first-pass extraction fraction of 80%, enabling myocardial perfusion and coronary flow reserve (myocardial perfusion reserve) to be evaluated quantitatively by compartment analysis. Stress is applied pharmacologically, and data for compartment analysis are collected by dynamic imaging (dynamic PET) in list mode. However, because a cyclotron is required, the facilities where it can be performed are limited. ^{18}F -flurpiridaz, the most recently developed agent, has a shorter positron range than ^{13}N and a high first-pass extraction fraction of $\geq 90\%$. Consequently, it is superior to ^{13}N -ammonia with respect to image quality and quantitative evaluation.⁵⁶⁾ Moreover, its long half-life of 110 minutes enables exercise stress testing to be performed, and because it can be supplied by delivery, it offers the advantage of enabling any PET facility to perform the test. Furthermore, because redistribution is observed, testing can be performed using the same test protocol used for ^{201}Tl .^{56, 57)} It is an agent whose future clinical introduction is eagerly awaited.

3. Myocardial metabolic imaging methods

The energy metabolism of the myocardium is mainly provided by fatty acids in the fasted state and glucose postprandially or during ischemia. The ^{123}I -labeled fatty acid analog ^{123}I -BMIPP is used to evaluate fatty acid metabolism, and ^{18}F -FDG is used to evaluate glucose metabolism. Although ^{123}I -BMIPP is taken up by the myocardium as a fatty acid, it is sequestered in the triglyceride pool without undergoing beta-oxidation, and it reflects the status of fatty acid utilization and the size of the triglyceride pool. ^{18}F -FDG is taken up by the myocardium by active transport via the glucose transporters (GLUT) and converted to ^{18}F -FDG-phosphate by hexokinase. It is not metabolized subsequently and is therefore sequestered in the myocardium. Clinically, ^{123}I -BMIPP is useful for diagnosing acute coronary syndrome (unstable angina) and predicting cardiovascular events in patients with chronic kidney disease (CKD) (cardiomyopathy, Table 2). ^{123}I -BMIPP is also used to evaluate myocardial viability during myocardial perfusion imaging and aspects such as myocardial damage in hypertrophic cardiomyopathy.⁵⁰⁾ ^{18}F -FDG is used to evaluate myocardial viability.^{50, 55)}

① ^{18}F -FDG imaging methods

Because GLUT4 is insulin-dependent, an insulin clamp, which involves the combined use of glucose loading and insulin, is used to evaluate the viability of the myocardium. Imaging is generally performed 45 to 60 minutes after administration of 5 to 15 mCi (185 to 555 MBq) of ^{18}F -FDG. Data are collected in static or list mode over an imaging duration of 10 to 30 minutes. Images are reconstructed using the iterative

reconstruction or FBP method with a slice thickness of 2 to 4 mm. Myocardial viability is evaluated in conjunction with myocardial perfusion imaging. The myocardium can be concluded to be viable in an area of decreased myocardial perfusion if ^{18}F -FDG accumulation is observed.⁵⁵⁾ Fasting is required as preparation to evaluate inflammatory disorders such as sarcoidosis.⁵⁵⁾

② ^{123}I -BMIPP imaging methods

With the patient fasted and at rest, 3 to 4 mCi (111 to 148 MBq) of ^{123}I -BMIPP are injected intravenously, and SPECT is performed 20 to 30 minutes later. A symmetrical energy window with a width of 20% centering on an energy peak of 159 keV is specified, and data are collected with a 180-degree circular orbit from 45 degrees RAO to 45 degrees LPO. Imaging data are collected from 32 angles using a 64×64 matrix for 30 to 45 seconds per angle. The collimators used include low-energy high-resolution (LEHR), extended low-energy general purpose (ELEGP), and medium-energy general purpose (MEGP) collimators. With Anger type gamma cameras, simultaneous dual-isotope imaging in combination with ^{201}Tl has been performed to simultaneously evaluate myocardial perfusion.⁵⁰⁾ However, CZT gamma cameras provide superior energy resolution, making simultaneous dual isotope collection with the myocardial perfusion agent $^{99\text{m}}\text{Tc}$ possible as well.⁵⁸⁾ It should be noted, however, that simultaneous dual-isotope collection requires crosstalk correction and increases the radiation exposure.

4. Cardiac sympathetic imaging

^{123}I -MIBG is used for cardiac sympathetic imaging. Unlike noradrenaline, ^{123}I -MIBG is not metabolized by enzymes such as the monoamine oxidases. However, like noradrenaline, it is taken into the presynaptic nerves by the uptake-1 transporter, enabling accumulation in the cardiac sympathetic preganglionic fibers to be imaged. Regions of interest are specified for the heart (H) and mediastinum (M) in frontal planar images, and the heart/mediastinum ratio (H/M ratio) and washout rate are calculated. In patients with heart failure in which cardiac function is decreased, including those with concomitant coronary artery disease, the late-phase images' H/M ratios and washout rate are both useful indices as predictors for cardiac events.⁵⁰⁾

^{123}I -MIBG imaging methods

In preparation for imaging, antidepressants, antipsychotics, and calcium channel blockers, which affect ^{123}I -MIBG accumulation, are withdrawn for 24 hours. In Japan, a variety of collimators are used, as is the case with ^{123}I -BMIPP, 111 MBq of ^{123}I -MIBG is administered, and frontal planar images and myocardial SPECT images are acquired approximately 15 to 30 minutes (early-phase images) and 3 to 4 hours (late-phase images) after administration.⁵⁰⁾ Also in Japan, the H/M ratio is calculated using software that converts each measured value to the value obtained with a MEGP collimator, which makes it possible to compare H/M ratios obtained with different collimators and systems.⁵⁹⁾

Secondary source materials used as references

- 1) Hecht HS et al: Journal of Cardiovascular Computed Tomography 2016 SCCT/STR guidelines for coronary artery calcium scoring of noncontrast noncardiac chest CT scans: a report of the Society of Cardiovascular Computed Tomography and Society of Thoracic Radiology. *J Cardiovasc Comput Tomogr* 11: 74-84, 2017
- 2) Halliburton SS et al: SCCT guidelines on radiation dose and dose-optimization strategies in cardiovascular CT 5: 198-224, 2011
- 3) Taylor AJ et al: ACCF/SCCT/ACR/AHA/ASE/ASNC/NASCI/SCAI/SCMR 2010 Appropriate Use Criteria for cardiac computed tomography. *J Cardiovasc Comput Tomogr* 4: 407.e1-407.e33, 2010
- 4) Abbara S et al: SCCT guidelines for the performance and acquisition of coronary computed tomographic angiography: a report of the Society of Cardiovascular Computed Tomography Guidelines Committee endorsed by the North American Society for Cardiovascular Imaging (NASCI). *J Cardiovasc Comput Tomogr* 10: 435-449, 2016
- 5) Utsunomiya D et al: Relationship between diverse patient body size- and image acquisition-related factors, and quantitative and qualitative image quality in coronary computed tomography angiography: a multicenter observational study. *Jpn J Radio* 34: 548-55, 2016
- 6) Gonzalez JA et al: Meta-analysis of diagnostic performance of coronary computed tomography angiography, computed tomography perfusion, and computed tomography-fractional flow reserve in functional myocardial ischemia assessment versus invasive fractional flow reserve. *Am J Cardiol* 116: 1469-1478, 2015
- 7) Nørgaard BL et al: Diagnostic performance of noninvasive fractional flow reserve derived from coronary computed tomography angiography in suspected coronary artery disease: The NXT trial (Analysis of Coronary Blood Flow Using CT Angiography: Next Steps). *J Am Coll Cardiol* 63: 1145-1155, 2014
- 8) Japanese Circulation Society, et al. Ed.: JCS 2018 Guideline on Diagnosis of Chronic Coronary Heart Diseases. Japanese Circulation Society, 2018.
- 9) Japanese Circulation Society, et al. Ed.: 2010 Guidelines on Selection Criteria for Testing Methods for Diagnosis and Pathology Identification in Chronic Ischemic Heart Disease. Japanese Circulation Society (JSC 2010), 2010.
- 10) Kramer CM et al: Society for Cardiovascular Magnetic Resonance Board of Trustees Task Force on Standardized Protocols.: standardized cardiovascular magnetic resonance (CMR) protocols 2020 update. *J Cardiovasc Magn Reson* 15, doi: 10.1186/s12968-020-00607-1/2020
- 11) Axel L, Dougherty L: Heart wall motion: improved method of spatial modulation of magnetization for MR imaging. *Radiology* 172: 349-350, 1989
- 12) Eitel I et al: Cardiac magnetic resonance myocardial feature tracking for optimized prediction of cardiovascular events following myocardial infarction. *JACC Cardiovasc Imaging* 11: 1433-1444, 2018
- 13) Nagel E et al: Magnetic resonance perfusion measurements for the noninvasive detection of coronary artery disease. *Circulation* 108: 432-437, 2003
- 14) Schwitzer J et al: MR-IMPACT: comparison of perfusion-cardiac magnetic resonance with single-photon emission computed tomography for the detection of coronary artery disease in a multicentre, multivendor, randomized trial. *Eur Heart J* 29: 480-489, 2008
- 15) Wagner A et al: Contrast-enhanced MRI and routine single photon emission computed tomography (SPECT) perfusion imaging for detection of subendocardial myocardial infarcts: an imaging study. *Lancet* 361: 374-379, 2003
- 16) Kim RJ et al: The use of contrast-enhanced magnetic resonance imaging to identify reversible myocardial dysfunction. *N Eng J Med* 343: 1445-1453, 2000
- 17) Weber OM et al: Whole-heart steady-state free precession coronary artery magnetic resonance angiography. *Magn Reson Med* 50: 1223-1228, 2003
- 18) Sakuma H et al: Assessment of the entire coronary artery tree with total study time of less than 30 minutes using whole heart coronary magnetic resonance angiography. *Radiology* 237: 316-321, 2005
- 19) Dyverfeldt P et al: 4D flow cardiovascular magnetic resonance consensus statement. *J Cardiovasc Magn* 17: 72, 2015
- 20) Roujol S et al: Accuracy, precision, and reproducibility of four T1 mapping sequences: a head-to-head comparison of MOLLI, ShMOLLI, SASHA, and SAPHIRE. *Radiology* 272: 683-689, 2014
- 21) Japanese Circulation Society, et al. Ed.: Guidelines for the Diagnosis and Treatment of Cardiovascular Disease (2010 report of the joint working group), 2011 Guideline on Diagnosis and Treatment of Aortic Aneurysm and Aortic Dissection. Japanese Circulation Society, 2011.
- 22) Prince MR: Gadolinium-enhanced MR aortography. *Radiology* 191: 155-164, 1994
- 23) Makris GC et al: Advances in MRI for the evaluation of carotid atherosclerosis. *B J Radiol* 88: 20140208, 2015
- 24) Ho KY et al: Peripheral vascular tree stenosis; evaluation with moving-bed infusion-tracking MR angiography. *Radiology* 206: 683-692, 1998
- 25) Miyazaki M et al: Non-contrast enhanced MR angiography using 3D ECG synchronized half-Fourier fast spin echo. *JMRI* 12: 776-783, 2000
- 26) Simonetti OP et al: "Black blood T2-weighted inversion-recovery MR imaging of the heart. *Radiology* 199: 49-57, 1996
- 27) Meaney TF et al: Digital subtraction angiography of the human cardiovascular system. *AJR Am J Roentgenol* 135 (6): 1153-1160, 1980
- 28) Malden ES et al: Peripheral vascular disease: evaluation with stepping DSA and conventional screen-film angiography. *Radiology* 191 (1): 149-153, 1994

- 29) Fink U et al: Peripheral DSA with automated stepping. *Eur J Radiol* 13 (1): 50-54, 1991
- 30) Foley WD et al: Digital subtraction angiography of the extremities using table translation. *Radiolog* 157 (1): 255-258, 1985
- 31) Kumazaki T: Development of a new digital angiography system--improvement of rotational angiography and three dimensional image display. *Nihon Igaku Hoshasen Gakkai Zasshi* 51 (9): 1068-1077, 1991
- 32) Heautot JF et al: Analysis of cerebrovascular diseases by a new 3-dimensional computerised X-ray angiography system. *Neuroradiology* 40 (4): 203-209, 1998
- 33) Wiesent K et al: Enhanced 3-D-reconstruction algorithm for C-arm systems suitable for interventional procedures. *IEEE Trans Med Imaging* 19 (5): 391-403, 2000
- 34) Buscaglia LC et al: Use of CT scan in the diagnosis of abdominal aortic aneurysms. *J Comput Tomogr* 4 (3): 197-200, 1980
- 35) Wheeler WE et al: Angiography and ultrasonography: a comparative study of abdominal aortic aneurysms. *AJR Am J Roentgenol* 126 (1): 95-100, 1976
- 36) Godwin JD et al: Evaluation of dissections and aneurysms of the thoracic aorta by conventional and dynamic CT scanning. *Radiology* 136 (1): 125-133, 1980
- 37) Heiberg E et al: CT findings in thoracic aortic dissection. *AJR Am J Roentgenol* 136 (1): 13-17, 1981
- 38) Tennant WG et al: Radiologic investigation of abdominal aortic aneurysm disease: comparison of three modalities in staging and the detection of inflammatory change. *J Vasc Surg* 17 (4): 703-709, 1993
- 39) Arrive L et al: Inflammatory aneurysms of the abdominal aorta: CT findings. *AJR Am J Roentgenol* 165 (6): 1481-1484, 1995
- 40) Iino M et al: Sensitivity and specificity of CT in the diagnosis of inflammatory abdominal aortic aneurysms. *J Comput Assist Tomogr* 26 (6): 1006-1012, 2002
- 41) Gotway MB et al: Imaging findings in Takayasu's arteritis. *AJR Am J Roentgenol* 184 (6): 1945-1950, 2005
- 42) Matsunaga N et al: Takayasu arteritis: MR manifestations and diagnosis of acute and chronic phase. *J Magn Reson Imaging* 8 (2): 406-414, 1998
- 43) Katz DS et al: Combined CT venography and pulmonary angiography: a comprehensive review. *Radiographics* 22: S3-S19 (S20-S14), 2002
- 44) Mills JL: Buerger's disease in the 21st century: diagnosis, clinical features, and therapy. *Semin Vasc Surg* 16 (3): 179-189, 2003
- 45) Hagen B, Lohse S: Clinical and radiologic aspects of Buerger's disease. *Cardiovasc Intervent Radiol* 7 (6): 283-293, 1984
- 46) Suzuki S et al: Buerger's disease (thromboangiitis obliterans): an analysis of the arteriograms of 119 cases. *Clin Radiol* 33 (2): 235-240, 1982
- 47) Henzlova MJ et al: ASNC imaging guidelines for SPECT nuclear cardiology procedures: stress, protocols, and tracers. *J Nucl Cardiol* 23: 606-639, 2016
- 48) Dorbala S et al: Single photon emission computed tomography (SPECT) myocardial perfusion imaging guidelines: instrumentation, acquisition, processing, and interpretation. *J Nucl Cardiol*. 25: 1784-1846, 2018
- 49) Gimelli A et al: Strategies for radiation dose reduction in nuclear cardiology and cardiac computed tomography imaging: a report from the European Association of Cardiovascular Imaging (EACVI), Committee of European Association of Nuclear Medicine (EANM), and the European Society of Cardiovascular Radiology (ESCR). *Eur Heart J* 39: 286-296, 2018
- 50) Yamagishi M, et al.: JCS 2018 Guideline on Diagnosis of Chronic Coronary Heart Diseases. JCS, 2018.
- 51) Travin MI et al: How do we establish cardiac sympathetic nervous system imaging with ¹²³I-MIBG in clinical practice? perspectives and lessons from Japan and the US. *J Nucl Cardiol* 26: 1434-1451. 2019
- 52) Dorbala S et al: ASNC/AHA/ASE/EANM/HFSA/ISA/SCMR/SNMMI expert consensus recommendations for multimodality imaging in cardiac amyloidosis: part 1 of 2-evidence base and standardized methods of imaging. *J Nucl Cardiol* 26: 2065- 2123. 2019
- 53) Slart RHJA et al: A joint procedural position statement on imaging in cardiac sarcoidosis: from The Cardiovascular and Inflammation & Infection Committees of European Association of Nuclear Medicine, The European Association of Cardiovascular Imaging, and the American Society of Nuclear Cardiology. *J Nucl Cardiol*. 25: 298-319, 2018
- 54) Saraste A et al: Imaging in ESC clinical guidelines: chronic coronary syndromes. *Eur Heart J* 20: 1187-1197, 2019
- 55) Dilsizian V et al: ASNC imaging guidelines/SNMMI procedure standard for positron emission tomography (PET) nuclear cardiology procedures. *J Nucl Cardiol* 23: 1187-1226, 2016
- 56) Werner RA et al: Moving into the next era of PET myocardial perfusion imaging: introduction of novel ¹⁸F-labeled tracers. *Int J Cardiovasc Imaging* 35: 569-577, 2019
- 57) Higuchi T et al: A new ¹⁸F-labeled myocardial PET tracer: myocardial uptake after permanent and transient coronary occlusion in rats. *J Nucl Med* 49: 1715-1722, 2008
- 58) Yamada Y et al: Feasibility of simultaneous ^{99m}Tc-tetrofosmin and ¹²³I-BMIPP dual-tracer imaging with cadmium-zinc-telluride detectors in patients undergoing primary coronary intervention for acute myocardial infarction. *J Nucl Cardiol*: DOI: 10.1007/s12350-018-01585-9, 2019
- 59) Nakajima K et al: Multicenter cross-calibration of I-123metaiodobenzylguanidine heart-to-mediastinum ratios to overcome camera-collimator variations. *J Nucl Cardiol* 21: 970-978, 2014

CQ 6 When \geq 64-row MDCT is used to investigate acute pulmonary thromboembolism, is simultaneous CT venography recommended?

Recommendation

Although CT venography (CTV) should not be uniformly performed with CT pulmonary angiography (CTPA) that is performed to investigate acute pulmonary thromboembolism, the combined use of CTV is considered when the lower extremities cannot be adequately observed by ultrasonography and when the risk of acute pulmonary thromboembolism is high.

Recommendation strength: none, strength of evidence: weak (C), agreement rate: agreement not reached

Background

The addition of CTV to CTPA improves diagnostic performance in acute pulmonary thromboembolism, according to a large study of \leq 16-row MDCT.¹⁾ It is not clear whether CTV is also needed with \geq 64-row MDCT or whether the addition of CTV is useful for determining a treatment strategy and contributes to prognosis improvement. The addition of CTV necessitates increased X-ray exposure and an increase in the dose of contrast medium. Consequently, the benefits and drawbacks need to be considered.

Explanation

Acute pulmonary thromboembolism requires prompt and accurate diagnosis. The diagnostic test is selected based on the pre-test probability (clinical probability). With a low to moderate clinical probability, CTPA is recommended to exclude acute pulmonary thromboembolism. With a moderate to high clinical probability, it is recommended to confirm acute pulmonary thromboembolism (secondary source 1). CTPA is now used as the reference standard for acute pulmonary embolism diagnosis, instead of direct catheter pulmonary angiography.

In a multicenter, prospective study that examined the diagnostic performance of CTPA using \leq 16-row MDCT [Prospective Investigation of Pulmonary Embolism Diagnosis (PIOPED) II trial], sensitivity and specificity were 83% and 96%, respectively. When simultaneous CTV was added, sensitivity and specificity improved to 90% and 95%, respectively. However, the availability of \geq 64-row MDCT has increased in recent years. Consequently, high diagnostic performance can be expected with CTPA alone. The number of studies that have examined whether the addition of CTV to CTPA using \geq 64-row MDCT contributes to improved diagnostic performance in acute pulmonary thromboembolism (venous thromboembolism) is limited.^{2,3)} Consequently, there is a lack of evidence supporting the clinical utility of additional CTV.

The embolic source in $\geq 90\%$ of patients with acute pulmonary thromboembolism is the deep veins of the lower extremities. Evaluation of the lower extremity deep venous thrombus is therefore necessary to determine a treatment strategy. The first-line imaging examination for evaluating lower extremity deep venous thrombus is ultrasonography of the lower extremities, which provides high diagnostic performance. Deep vein thrombosis that is localized in the pelvis is difficult to evaluate by ultrasound, and evaluation by CTV may be useful in this case. However, such cases are very rare.^{4,5)} Consequently, information obtained by CTV alone in the diagnosis of deep vein thrombosis is limited. The addition of CTV allows for incidental findings in the pelvis and lower extremities (e.g., tumors, abscesses, aneurysms), which may assist in determining a treatment strategy. However, this occurs infrequently, and the usefulness of CTV in this role is therefore limited.⁶⁾

The addition of CTV is accompanied by increased X-ray and contrast medium doses. Ultrasonography of the lower extremities should therefore generally be given priority in diagnosing deep vein thrombosis, and the use of CTV should be limited to cases in which evaluation of the lower extremities by ultrasonography is difficult (secondary sources 2 to 5). The addition of CTV to CTPA may enable ultrasonography of the lower extremities to be omitted in the following cases, thereby shortening the diagnostic process and aiding in promptly determining a treatment strategy: ultrasonography of the lower extremities cannot be properly performed at the facility; circumstances make it difficult to perform (e.g. postoperative site or a cast is in place); image evaluation by ultrasonography is difficult; or the patient is in a highly urgent condition (e.g., condition unstable or high risk).⁷⁾ However, the effects of adding CTV on healthcare management and prognosis have not been adequately investigated, which makes it difficult to comment on its usefulness.

None of the guidelines on acute pulmonary thromboembolism and deep vein thrombosis published in Japan or other countries recommend routinely adding CTV to CTPA. The view expressed in these guidelines is that the addition of CTV does not provide benefits commensurate with the increases in X-ray exposure and contrast medium dose, and that there is little evidence supporting the aggressive use of CTV (secondary sources 1-3, 6). The present guidelines also do not recommend the uniform use of CTV in combination with CTPA. However, it may assist in promptly determining a treatment strategy when adequate observation by lower extremity ultrasonography is not feasible or in high-risk patients. It was therefore concluded that concomitant CTV should remain an option after its benefits and drawbacks have been individually considered.

Search keywords and secondary sources used as references

PubMed was searched using the following keywords: deep vein thrombosis, deep venous thrombosis, venography, angiography, computed tomography angiography, pulmonary embolism, pulmonary thromboembolism, and venous thromboembolism.

In addition, the following were referenced as secondary sources.

- 1) Konstantinides SV et al: 2019 ESC guidelines for the diagnosis and management of acute pulmonary embolism developed in collaboration with the European Respiratory Society (ERS). *Eur Heart J* 41: 543-603, 2020

- 2) Mazzolai L et al. Diagnosis and management of acute deep vein thrombosis: a joint consensus document from The European Society of Cardiology working groups of aorta and peripheral vascular diseases and pulmonary circulation and right ventricular function. *Eur Heart J* 39: 4208-4218, 2018
- 3) Hanley M et al: ACR Appropriateness Criteria®: suspected lower extremity deep vein thrombosis. *J Am Coll Radiol* 15: S413-s417, 2018
- 4) Ito M, et al.: 2017 Guidelines for Diagnosis, Treatment and Prevention of Pulmonary Thromboembolism and Deep Vein Thrombosis. Japanese Circulation Society, 2017.
- 5) Japan Radiological Society, Ed.: 2016 Diagnostic Imaging Guideline. KANEHARA & Co., 2016.
- 6) Kirsch J et al: ACR Appropriateness Criteria®: acute chest pain-suspected pulmonary embolism. *J Am Coll Radiol* 14: S2-S12, 2017

References

- 1) Stein PD et al: Multidetector computed tomography for acute pulmonary embolism. *N Engl J Med* 354: 2317-2327, 2006
- 2) Nazarglu H et al: 64-MDCT pulmonary angiography and CT venography in the diagnosis of thromboembolic disease. *AJR Am J Roentgenol* 192: 654-661, 2009
- 3) Stein PD et al: CT venous phase venography with 64-detector CT angiography in the diagnosis of acute pulmonary embolism. *Clin Appl Thromb Hemost* 16: 422-429, 2010
- 4) Reichert M et al: Venous thromboembolism: additional diagnostic value and radiation dose of pelvic CT venography in patients with suspected pulmonary embolism. *Eur J Radiol* 80: 50-53, 2011
- 5) Kalva SP et al: Venous thromboembolism: indirect CT venography during CT pulmonary angiography--should the pelvis be imaged? *Radiology* 246: 605-611, 2008
- 6) Douek P et al: Impact of CT venography added to CT pulmonary angiography for the detection of deep venous thrombosis and relevant incidental CT findings. *Eur J Radiol* 133: 109388, 2020
- 7) Salvolini L et al: Suspected pulmonary embolism and deep venous thrombosis: a comprehensive MDCT diagnosis in the acute clinical setting. *Eur J Radiol* 65: 340-349, 2008

CQ 7 Is functional testing with FFR-CT recommended if intermediate stenosis is seen by coronary CTA performed for effort angina?

Recommendation

FFR-CT is weakly recommended as a functional test if intermediate stenosis is seen on coronary CTA performed to investigate effort angina.

Recommendation strength: 2, strength of evidence: weak (A), agreement rate: 80% (8/10)

Background

Fractional flow reserve (FFR) is a well-established test for determining the indication for coronary revascularization, but it requires pharmacological stress for each individual lesion. FFR derived from coronary CT angiography (FFR-CT) offers the advantage of evaluating the severity of myocardial ischemia for each diseased vessel assessable by coronary CTA without additional testing. However, the usefulness of coronary CTA in intermediate stenosis (30% to 70%) has not been adequately evaluated.

Explanation

In the diagnostic algorithm for chronic coronary artery disease, coronary CTA holds an important role as a noninvasive test, on a par with stress electrocardiography and stress myocardial perfusion imaging. However, coronary CTA is useful for excluding significant coronary artery stenoses ($\geq 50\%$), it is known to be inadequate for identifying obstructive coronary artery disease (CAD) requiring treatment. The invasive FFR is a well-established diagnostic examination for determining the indication for coronary revascularization, but it requires pharmacological stress-loading for each individual lesion. FFR-CT is a method of evaluation used to estimate the severity of myocardial ischemia for each diseased vessel (FFR). It does so using 3D data from coronary CTA and applying the fundamentals of computational fluid dynamics and cardiovascular physiology to hypothetically calculate pharmacological stress conditions.

For this CQ, we searched for studies that evaluated the diagnostic performance of coronary CTA (lesions of $\geq 50\%$ stenosis) and FFR-CT (≤ 0.80) with respect to obstructive CAD (invasive FFR ≤ 0.80) in patients who had undergone coronary CTA for suspected effort angina. We explored the CADs with stenosis severity of 30% to 70% on coronary CTA, which are difficult to manage after testing. We reviewed seven studies, consisting of five prospective and two retrospective studies and evaluated a total of 1,701 vessels as the study population.¹⁻⁷⁾ The studies were uniform with respect to entry requirements such as the intervals between CT and FFR tests, the definition of intermediate stenosis (30% to 70%), endpoint blinding, and outcome condition (invasive FFR ≤ 0.80).

The results of a quantitative meta-analysis of these studies are shown in Table 1. Sensitivity ranged from 0.34 to 0.90 for coronary CTA [pooled sensitivity, 0.71 (95% CI, 0.40 to 0.91)] and from 0.59 to 0.95 for FFR-CT [pooled sensitivity, 0.86 (95% CI, 0.83 to 0.91)]. Thus, the sensitivity of FFR-CT was

comparatively stable and high. Specificity ranged from 0.21 to 0.87 for coronary CTA [pooled specificity, 0.49 (95% CI, 0.18 to 0.81)] and from 0.59 to 0.95 for FFR-CT [pooled specificity, 0.80 (95% CI, 0.77 to 0.83)]. Thus, the specificity of FFR-CT also showed a trend toward being comparatively high. As compared with coronary CTA, FFR-CT had a higher positive likelihood ratio (PLR) [pooled PLR, 4.07 (95% CI, 2.49 to 6.66) vs. 1.24 (95% CI, 1.02 to 1.51)], a lower negative likelihood ratio (NLR) [pooled NLR, 0.18 (95% CI, 0.11 to 0.27) vs. 0.65 (95% CI, 0.45 to 0.93)], and a higher diagnostic odds ratio (DOR) [pooled DOR, 26.52 (95% CI, 10.42 to 67.49) vs. 2.30 (95% CI, 1.30 to 4.07)]. The area under the curve (AUC) of the summary receiver operating characteristic (SROC) was also larger for FFR-CT than for coronary CTA (Fig. 1, 0.9183 vs. 0.6487).

References 1 to 3 and 6 were studies that used analysis software made by HeartFlow. The remaining 3 studies used different computational algorithms to calculate FFR-CT (in Japan, only HeartFlow FFR-CT is reimbursed under national health insurance).^{4,5,7)} Previous studies have shown that FFR-CT improved the diagnostic performance of identifying obstructive CAD compared to coronary CTA alone, applying the same cutoff value.⁸⁾ In the systematic review for this CQ, the inconsistency of the results for the sensitivity of coronary CTA (I-square = 90.3%) and specificity (I-square = 96.1%) and for the sensitivity of FFR-CT (I-square = 92.9%) must be considered in the assessment.

Table. Diagnostic performance of coronary CTA ($\geq 50\%$) and FFR-CT (≤ 0.80) for vessels diagnosed as having intermediate stenosis (30% to 70% stenosis) by coronary CTA

	Number of Vessels	Number of Lesions	Sensitivity [95% CI]	Specificity [95% CI]	PLR [95% CI]	NLR [95% CI]	DOR [95% CI]
CCTA ($\geq 50\%$)							
Min 2012 ¹⁾	66	31	0.90 [0.74-0.98]	0.26 [0.13-0.43]	1.22 [0.97-1.53]	0.38 [0.11-1.27]	3.2 [0.79-13.25]
Nakazato 2013 ²⁾	150	35	0.34 [0.19-0.52]	0.72 [0.63-0.80]	1.23 [0.71-2.13]	0.91 [0.70-1.19]	1.35 [0.60-3.04]
Coenen 2015 ⁴⁾	144	63	0.83 [0.71-0.91]	0.21 [0.13-0.31]	1.05 [0.89-1.23]	0.83 [0.42-1.65]	1.26 [0.54-2.92]
Donnelly 2018 ⁵⁾	60	21	0.52 [0.30-0.74]	0.87 [0.73-0.96]	4.09 [1.64-10.20]	0.55 [0.34-0.87]	7.48 [2.10-26.65]
Tang 2020 ⁷⁾	299	76	0.84 [0.74-0.92]	0.35 [0.28-0.41]	1.29 [1.12-1.47]	0.46 [0.27-0.79]	2.81 [1.43-5.53]
pooled	719	226	0.71 [0.40-0.91]	0.49 [0.18-0.81]	1.24 [1.02-1.51]	0.65 [0.45-0.93]	2.30 [1.30-4.07]
FFR-CT (≤ 0.80)							
Min 2012 ¹⁾	66	31	0.9 [0.74-0.98]	0.83 [0.66-0.93]	5.27 [2.52-11.01]	0.18 [0.04-0.35]	45.11 [10.27-198.1]
Nakazato 2013 ²⁾	150	35	0.74 [0.57-0.88]	0.67 [0.58-0.75]	2.25 [1.62-3.11]	0.38 [0.22-0.68]	5.85 [2.50-13.72]
Nørgaard 2014 ³⁾	234	34	0.82 [0.66-0.93]	0.86 [0.80-0.90]	5.68 [3.92-8.23]	0.21 [0.10-0.43]	27.52 [10.48-72.27]
Coenen 2015 ⁴⁾	144	63	0.87 [0.77-0.94]	0.59 [0.48-0.70]	2.14 [1.62-2.83]	0.21 [0.11-0.42]	10.00 [4.22-23.73]
Donnelly 2018 ⁵⁾	60	21	0.91 [0.70-0.99]	0.72 [0.55-0.85]	3.21 [1.91-5.39]	0.13 [0.04-0.50]	24.18 [4.81-121.6]
Driessen 2019 ⁶⁾	118	50	0.96 [0.86-1.00]	0.66 [0.54-0.77]	2.84 [2.03-3.98]	0.06 [0.02-0.24]	46.96 [10.47-210.7]
Tang 2020 ⁷⁾	299	76	0.88 [0.79-0.94]	0.95 [0.91-0.98]	17.87 [9.99-31.99]	0.13 [0.07-0.23]	143.5 [57.02-361.0]
pooled	1071	310	0.87 [0.83-0.91]	0.80 [0.77-0.83]	4.07 [2.49-6.66]	0.18 [0.11-0.27]	26.52 [10.42-67.49]

Note: Invasive FFR ≤ 0.80 considered as reference standard.

FFR-CT can detect coronary lesions that require treatment with high diagnostic accuracy and without the need for additional testing (Fig. 2). In its expert consensus, the Society of Cardiovascular Computed Tomography of the United States stated that FFR-CT evaluation may optimize further examination after coronary CTA diagnosis and may help with decision-making in strategies for patients with severe single-vessel disease or multivessel disease that includes intermediate stenoses (secondary source 1).

However, the medical remuneration points for FFR-CT provided under the national health insurance system are not necessarily reasonable compared to coronary CTA. Consequently, if the clinical indication for FFR-CT as an additional test is not adequately considered, the number of FFR-CT analyses could increase and strain the economics of healthcare. Of course, we should know that FFR-CT may be affected

by a variety of factors, such as CT image quality, coronary artery calcification, and patient-related factors.⁹⁻¹¹⁾ The healthcare policies have allowed the use of FFR-CT analysis in the approved hospitals that can appropriately operate and evaluate coronary CTA, to avoid increases in medical costs. The Japanese Circulation Society (JCS) working group recently collaborated with related academic societies and proposed the appropriate use criteria for FFR-CT. The appropriate use criteria stipulate details such as the facility requirements established by the relevant societies and the use of FFR-CT only for CAD with $\geq 50\%$ stenosis on coronary CTA (secondary source 2). The Japanese Circulation Society's 2018 Guideline on Diagnosis of Chronic Coronary Heart Diseases took into account guidelines on the appropriate use of FFR-CT and the status of its use in Japan and provided recommendations for its clinical use that are of recommendation class IIb and evidence level B (MINDS recommendation grade B and evidence classification II; secondary source 3).

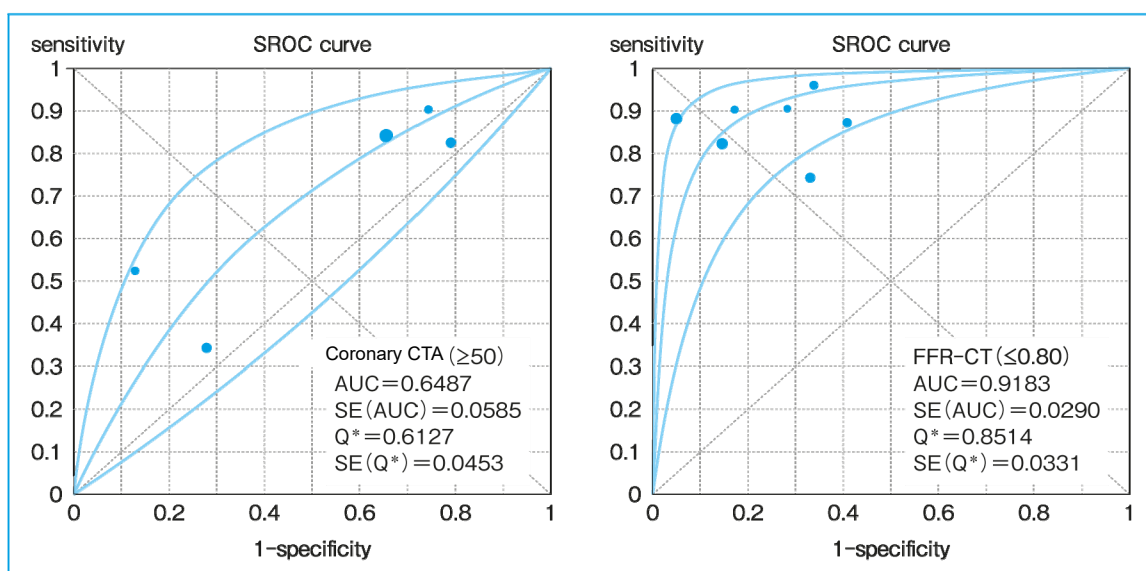


Figure 1. SROCs for coronary CTA ($\geq 50\%$) and FFR-CT (≤ 0.80)

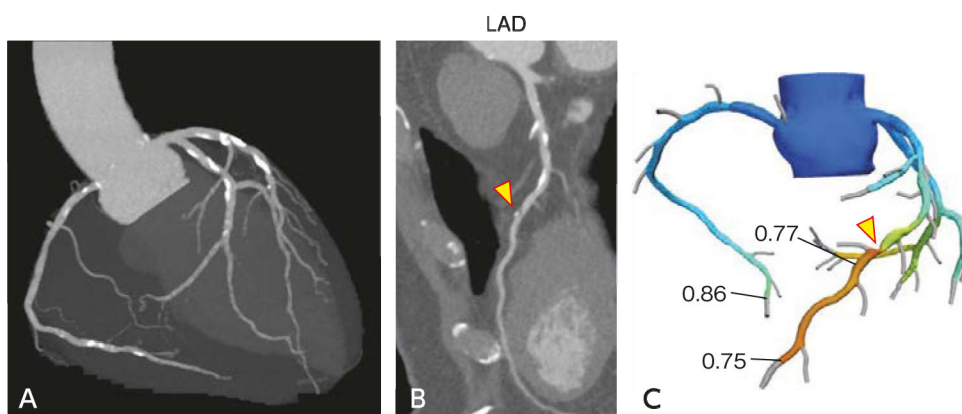


Figure 2. Clinical case with additional FFR-CT analysis

The patient was a man in his 60s. Multiple moderate stenoses are seen in the left anterior descending artery (LAD) on coronary CTA. An FFR-CT analysis was therefore performed (A, B). An FFR-CT value of 0.77 was obtained for the distal stenotic lesion with minor calcification in the distal LAD (C).

Some studies and systematic reviews have found that FFR-CT values near 0.8 had a grey zone of diagnostic accuracy with wide confidence intervals, false positives, and false negatives.^{12, 13)} The current appropriate use criteria in Japan allow FFR-CT only to assess CAD with stenosis $\geq 50\%$ on coronary CTA. Consequently, the present meta-analyses, including some vessels with 30% to 49% stenosis, may not be optimal for this CQ. A previous study reported that approximately 80% of vessels with stenosis of 30% to 49% have an FFR-CT value > 0.8 .¹⁴⁾ In this regard, it may be necessary to consider that the evaluation of FFR-CT diagnostic performance in the systematic review conducted for this CQ is a slight underestimate. In addition, a point to keep in mind when using FFR-CT clinically is that the national healthcare insurance system will not cover part of the medical costs for the downstream tests after FFR-CT analysis according to the supplementary items for clinical use of FFR-CT. For instance, this regulation will be applied when the cases undergo FFR-CT analysis, invasive FFR, and stress MPI using nuclear or magnetic resonance imaging in a series of further investigations for obstructive CAD.

Search keywords and secondary sources used as references

PubMed was searched using the following keywords: computed tomography, fractional flow reserve, FFR, intermediate stenosis, myocardial, coronary computed tomographic, coronary CT, stenosis, computed tomography angiography, and sensitivity.

In addition, the following were referenced as secondary sources.

- 1) Narula N et al: SCCT 2021 expert consensus document on coronary computed tomographic angiography: a report of the Society of Cardiovascular Computed Tomography. *J Cardiovasc Comput Tomogr.* S1934-5925: 30473-30471, 2021
- 2) Japanese Circulation Society Task Force Committee: Guidelines on the Appropriate Use of FFRCT, revised on December 1, 2018. Japanese Circulation Society, 2018.
- 3) Japanese Circulation Society, Ed.: Guidelines for the diagnosis and treatment of cardiovascular disease: JCS 2018 Guideline on Diagnosis of Chronic Coronary Heart Diseases. Japanese Circulation Society, 2009.

References

- 1) Min JK et al: Usefulness of noninvasive fractional flow reserve computed from coronary computed tomographic angiograms for intermediate stenoses confirmed by quantitative coronary angiography. *Am J Cardiol* 110: 971-976, 2012
- 2) Nakazato R et al: Noninvasive fractional flow reserve derived from computed tomography angiography for coronary lesions of intermediate stenosis severity: results from the DeFACTO study. *Circ Cardiovasc Imaging* 6: 881-889, 2013
- 3) Nørgaard BL et al: Diagnostic performance of noninvasive fractional flow reserve derived from coronary computed tomography angiography in suspected coronary artery disease: the NXT trial (analysis of coronary blood flow using CT angiography: next steps). *J Am Coll Cardiol* 63: 1145-1155, 2014
- 4) Coenen A et al: Fractional flow reserve computed from noninvasive CT angiography data: diagnostic performance of an on-site clinician-operated computational fluid dynamics algorithm. *Radiology* 274: 674-83, 2015
- 5) Donnelly PM et al: Experience with an on-site coronary computed tomography-derived fractional flow reserve algorithm for the assessment of intermediate coronary stenoses. *Am J Cardiol* 121: 9-13, 2018
- 6) Driessen RS et al: Comparison of coronary computed tomography angiography, fractional flow reserve, and perfusion imaging for ischemia diagnosis. *J Am Coll Cardiol Img* 73: 161-173, 2019
- 7) Tang CX et al: CT FFR for ischemia-specific CAD with a new computational fluid dynamics algorithm: a chinese multicenter study. *JACC Cardiovasc Imaging*: 13: 980-990, 2020
- 8) Zhuang B et al: Computed tomography angiography-derived fractional flow reserve (CT-FFR) for the detection of myocardial ischemia with invasive fractional flow reserve as reference: systematic review and meta-analysis. *Eur Radiol.*30: 712-725, 2020

- 9) Nørgaard BL et al: Influence of coronary calcification on the diagnostic performance of CT angiography derived FFR in coronary artery disease: a substudy of the NXT trial. *JACC Cardiovasc Imaging* 8: 1045-1055, 2015
- 10) Takx AP et al: Sublingual nitroglycerin administration in coronary computed tomography angiography: a systematic review. *Eur Radiol*. 25: 3536-42, 2015
- 11) Coenen A et al: Coronary CT angiography derived fractional flow reserve: Methodology and evaluation of a point of care algorithm. *J Cardiovasc Comput Tomogr* 10: 105-113, 2016
- 12) Cook CM et al: Diagnostic accuracy of computed tomography-derived fractional flow reserve: a systematic review. *JAMA Cardiol* 2: 803-810, 2017
- 13) Coenen A et al: Diagnostic accuracy of a machine-learning approach to coronary computed tomographic angiography-based fractional flow reserve: result from the MACHINE consortium. *Circ Cardiovasc Imaging* 11: e007217, 2018
- 14) Kitabata H et al: Incidence and predictors of lesion-specific ischemia by FFR CT: learnings from the international ADVANCE registry. *J Cardiovasc Comput Tomogr* 12: 95-100, 2018

CQ 8 Is MRI T1 mapping recommended for diagnosing left ventricular hypertrophy?

Recommendation

MRI T1 mapping is weakly recommended for diagnosing left ventricular hypertrophy.

Recommendation strength: 2, strength of evidence: weak (C), agreement rate: 83% (10/12)

Background

The diseases that result in left ventricular hypertrophy are varied, but mainly include cardiomyopathy, such as hypertrophic cardiomyopathy, Fabry disease, cardiac amyloidosis, and hypertensive heart disease. Cine MRI and late gadolinium enhanced (LGE) MRI are imaging modalities with established evidence levels for the diagnosis of cardiomyopathy. However, in patients with suspected cardiomyopathy and left ventricular hypertrophy, there are limits to the ability of those conventional cardiac MRI techniques alone to diagnose the cause of left ventricular hypertrophy. Consequently, the systematic review conducted for this CQ examined whether T1 mapping with conventional cine MRI or LGE MRI provides added value in diagnosing the underlying etiology of left ventricular hypertrophy in patients with suspected cardiomyopathy and left ventricular hypertrophy.

Explanation

In preparing the recommendation for this CQ, the following 3 outcomes were specified with regard to whether T1 mapping with conventional cine MRI or LGE MRI provides added value in diagnosing the underlying etiology of left ventricular hypertrophy in patients with suspected cardiomyopathy and left ventricular hypertrophy: diagnosis of cardiac amyloidosis; differentiation between hypertrophic cardiomyopathy and hypertensive cardiac hypertrophy; and differentiation between Fabry disease and hypertrophic cardiomyopathy.

Three studies that examined cardiac amyloidosis consistently found strikingly high myocardial T1 values in cardiac amyloidosis and that myocardial T1 was therefore of high diagnostic value.¹⁻³⁾ In a case-control study, Karamitsos et al. performed T1 mapping using the shortened modified look-locker inversion recovery (ShMOLLI) (1.5T) in 53 patients with AL amyloidosis (with no cardiac involvement, n = 14; with possible cardiac involvement, n = 11; and with definite cardiac involvement, n = 28), 17 patients with aortic stenosis, and 36 healthy individuals.¹⁾ The results showed that myocardial T1 values were significantly higher in patients with cardiac amyloidosis than in healthy individuals (1,140 ± 61 ms vs. 958 ± 20 ms, p < 0.001). In a receiver-operating characteristic (ROC) curve analysis of these patient groups, those suspected of having cardiac amyloidosis and those with cardiac amyloidosis were considered positive for cardiac amyloidosis, and the remainder were considered negative. The resulting AUC was 0.97 (p < 0.0001), and the cutoff was 1,020 ms. In a case-control study by Fontana et al., T1 mapping using ShMOLLI (1.5T) was

performed in patients with transthyretin (ATTR) cardiac amyloidosis (n = 85), healthy individuals with a transthyretin gene abnormality (n = 8), patients with light-chain (AL) cardiac amyloidosis (n = 79), patients with hypertrophic cardiomyopathy (n = 46), and healthy individuals (n = 52).²⁾ The study found that myocardial T1 values were significantly higher in patients with ATTR cardiac amyloidosis than in those with hypertrophic cardiomyopathy or healthy individuals (1,097 ± 43 ms, 1,026 ± 64 ms, and 967 ± 34 ms, respectively; p < 0.0001 for both differences). Moreover, diagnostic performance with respect to hypertrophic cardiomyopathy was comparably high for both AL cardiac amyloidosis and ATTR cardiac amyloidosis [The AUC for diagnostic performance was 0.84 (95% CI, 0.76 to 0.92) in accurately differentiating between AL cardiac amyloidosis and hypertrophic cardiomyopathy and 0.85 (95% CI, 0.77 to 0.92) in accurately differentiating between ATTR cardiac amyloidosis and hypertrophic cardiomyopathy; p < 0.0001 for both]. A large cohort study by Baggiano et al. involving patients with suspected cardiac amyloidosis (n = 868) found that myocardial T1 values (modified look-locker inversion recovery (MOLLI), 1.5T) were significantly higher in patients whose final diagnosis was cardiac amyloidosis (n = 441) than in the other patients (n = 427; 1,149 ± 63 ms vs. 1,038 ± 50 ms, p < 0.001).³⁾ An ROC analysis showed the diagnostic accuracy of myocardial T1 for cardiac amyloidosis to be high (AUC = 0.93). When myocardial T1 was < 1,036 ms, cardiac amyloidosis could be excluded with a negative predictive value of 98%; when myocardial T1 was ≥ 1,164 ms, cardiac amyloidosis could be diagnosed with a positive predictive value of 98%. The same study found the diagnostic performance of myocardial T1 in cardiac amyloidosis to be significantly higher than that of indices obtained with conventional cine MRI and delayed contrast-enhanced MRI. Moreover, a between-groups comparison according to the presence or absence of left ventricular hypertrophy showed no difference in the diagnostic performance of myocardial T1 in cardiac amyloidosis (p = 0.35).

With regard to distinguishing between hypertrophic cardiomyopathy and hypertensive cardiac hypertrophy, a case-control study by Hinojar et al. was included in the review.⁴⁾ In that study, T1 mapping was performed using MOLLI (3.0T) in patients with hypertrophic cardiomyopathy (n = 95), hypertensive cardiac hypertrophy (n = 69), hypertrophic cardiomyopathy genotype positive/phenotype negative (n = 23), and healthy individuals (n = 23). Myocardial T1 values were significantly higher in hypertrophic cardiomyopathy than in hypertensive cardiac hypertrophy (1,169 ± 41 ms vs. 1,058 ± 29 ms, p < 0.05). Moreover, myocardial T1 showed extremely high sensitivity and specificity in distinguishing between hypertrophic cardiomyopathy and hypertensive cardiac hypertrophy, with sensitivity of 96% (95% CI, 87% to 99%) and specificity of 98% (95% CI, 92% to 100%).

Two case-control studies concerned with distinguishing between Fabry disease and hypertrophic cardiomyopathy were included in the review.^{5,6)} They found the low myocardial T1 values seen in Fabry disease to be of high diagnostic value. Karur et al. performed T1 mapping using MOLLI (3.0T) in patients with Fabry disease (n = 30) and hypertrophic cardiomyopathy (n = 30).⁵⁾ They found myocardial T1 values to be significantly lower in Fabry disease than in hypertrophic cardiomyopathy (1,161 ± 47 ms vs 1,296 ± 55 ms, p < 0.001). Using a cutoff of 1,220 ms, Fabry disease could be distinguished from hypertrophic

cardiomyopathy with sensitivity and specificity of 97% and 93%, respectively. DeBore et al. performed T1 mapping using MOLLI (1.5T) in patients with Fabry disease (n = 17) and hypertrophic cardiomyopathy (n = 36) and healthy individuals (n = 70).⁶⁾ The results showed that myocardial T1 was significantly lower in patients with Fabry disease (891 ± 49 ms) than in those with hypertrophic cardiomyopathy (995 ± 34 ms) and healthy controls (966 ± 27 ms; p < 0.001 for both). Moreover, using a cutoff of 940 ms, Fabry disease could be distinguished from hypertrophic cardiomyopathy with sensitivity and specificity of 88% and 92%, respectively.

A problem common to the above studies included in the review is that the results shown are those obtained with an optimal threshold value for each group of study subjects, and it is unclear whether they are applicable to other facilities. In addition, the studies did not examine the added value to cine MRI and LGE MRI in differentiating between hypertrophic cardiomyopathy and hypertensive cardiac hypertrophy and between Fabry disease and hypertrophic cardiomyopathy.⁴⁻⁶⁾ Furthermore, the patients included in the studies that examined cardiac amyloidosis diagnosis and the differentiation of Fabry disease and hypertrophic cardiomyopathy did not always have left ventricular hypertrophy.^{1,2,5,6)} Based on the above considerations, it was concluded that the evidence that it is useful to add T1 mapping to MRI in patients with left ventricular hypertrophy is weak. However, the addition of T1 mapping is likely to improve diagnostic accuracy in cardiac amyloidosis and Fabry disease and could greatly affect treatment strategy decisions. Moreover, T1 mapping is not invasive and does not clearly increase the cost of testing, aside from prolonging test duration to a certain extent. In view of these considerations, it is weakly recommended that T1 mapping be performed.

Search keywords and secondary sources used as references

PubMed was searched using the following keywords: hypertrophy, left ventricular, LVH, hypertrophies, hypertrophic cardiomyopathy, cardiomyopathy, hypertrophic, Fabry disease, immunoglobulin light-chain amyloidosis, hereditary amyloidosis, amyloidosis, familial, late gadolinium enhancement, magnetic resonance imaging, T1, T1 map, and T1 mapping. Eighty-two articles were extracted. A systematic review was conducted, and 6 articles that clearly indicated sensitivity and specificity were ultimately included.

References

- 1) Karamitsos TD et al: Noncontrast T1 mapping for the diagnosis of cardiac amyloidosis. *JACC Cardiovasc Imaging* 6: 488-497, 2013
- 2) Fontana M et al: Native T1 mapping in transthyretin amyloidosis. *JACC Cardiovasc Imaging*: 157-165, 2014
- 3) Baggiano A et al: Noncontrast magnetic resonance for the diagnosis of cardiac amyloidosis. *JACC Cardiovasc Imaging* 13: 69-80, 2020
- 4) Hinojar R et al: T1 mapping in discrimination of hypertrophic phenotypes: hypertensive heart disease and hypertrophic cardiomyopathy: findings from the international T1 multicenter cardiovascular magnetic resonance study. *Circ Cardiovasc Imaging* 8: e003285, 2015
- 5) Karur GR et al: Use of myocardial T1 mapping at 3.0 T to differentiate Anderson-Fabry disease from hypertrophic cardiomyopathy. *Radiology* 288: 398-406, 2018
- 6) Deborde E et al: Differentiation between Fabry disease and hypertrophic cardiomyopathy with cardiac T1 mapping. *Diagn Interv Imaging* 101: 59-67, 2020

BQ 33 Are CT and MRI recommended for diagnosing Takayasu's arteritis?

Statement

Contrast-enhanced CT is useful and recommended.

If contrast-enhanced CT is difficult to implement, MRI, which provides comparable diagnostic performance, is recommended. MRI, which does not involve radiation exposure, is preferable for long-term follow-up observation.

Background

Pathological diagnosis is rarely performed for the definitive diagnosis of Takayasu arteritis. It is generally diagnosed through a comprehensive assessment of factors such as imaging findings, the patient's clinical course, and test findings. Diagnostic imaging plays a particularly important role in diagnosing this condition. Accurate diagnostic imaging makes it possible to diagnose the condition early and begin appropriate treatment.

Explanation

Takayasu arteritis is a nonspecific, idiopathic vasculitis that affects elastic vessels such as the aorta, its major branches, and the pulmonary artery. It is common in Japan and other Asian countries and commonly occurs in young to middle-aged women. The patients it affects are often included in a patient group with fever of unknown origin. When young women present with complaints of fever and malaise, it is important to keep Takayasu arteritis in mind during differential diagnosis.

1. Diagnostic overview

The diagnostic criteria for Japan [Guidelines for Management of Vasculitis Syndrome (JCS 2017)] state that definitive diagnosis centers on diagnostic imaging (CT, MRI ultrasound, PET/CT, chest radiography, and angiography; secondary source 1). The morphology of the aorta and its main branches can be adequately evaluated with recent CT and MRI systems, and these modalities are recommended for the initial evaluation of Takayasu arteritis (secondary source 2).

Takayasu arteritis is associated with the following characteristic diagnostic imaging findings, and its diagnosis can be considered definitive if one or more of the symptoms indicated in the guidelines are present: multiple or diffuse hypertrophic, stenotic (including occlusions), or dilated lesions (including aneurysms) in the aorta and/or its primary branches. However, the following conditions must be excluded for definitive diagnosis: ① arteriosclerosis, ② a congenital vascular anomaly, ③ inflammatory abdominal aortic aneurysm, ④ infected aneurysm, ⑤ syphilitic aortitis, ⑥ giant cell arteritis (temporal arteritis), ⑦ vascular Behçet's disease, and ⑧ IgG4-related disease.

2. Usefulness of CT and MRI in the acute phase

The previous gold standard for diagnostic imaging of this condition was digital subtraction angiography (DSA).¹⁾ However, although DSA is an excellent method of evaluating the vessel lumen for conditions such as stenosis and dilatation, it is not suitable for evaluating the wall thickening without luminal changes that is seen in the acute phase. Consequently, the initial diagnosis of Takayasu arteritis is now almost always performed by CT and MRI. Thickening of the full circumference of the aortic wall is a characteristic of the acute phase. On non-contrast CT, the thickened aortic wall is seen as a hyperintensity area. In the late phase of contrast-enhanced CT, nearly homogeneous enhancement is seen in the thickened wall. However, double-ring-shaped enhancement may be seen on careful observation.²⁻⁶⁾ This double-ring-shaped enhancement is called the double ring-like sign. The outer layer of contrast enhancement is thought to reflect inflammatory changes associated with angiogenesis of the vascular media and adventitia. The inner layer, which shows weak contrast enhancement, is thought to correspond to mucinous and gelatinous swelling of the intima. The frequency of pulmonary artery lesions in this condition is relatively high, approximately 70% to 80%. Consequently, its presence or absence may be the deciding factor in differentiating Takayasu arteritis from other diseases. Attention must therefore also be paid to pulmonary artery wall thickening and contrast enhancement in the acute phase.⁶⁾ Similar acute-phase wall thickening and enhancement are also seen on contrast-enhanced MRI. Consequently, MRI, which does not involve radiation exposure, is useful for evaluating treatment efficacy and long-term follow-up observation.⁷⁻⁹⁾ If Takayasu arteritis is diagnosed and corticosteroid therapy is started in this phase, improvement in arterial wall thickening is likely. However, nonspecific inflammatory findings such as fever of unknown origin are often the only changes seen clinically, and it is often not appropriately diagnosed.



Figure 1. Takayasu arteritis (acute phase: woman in her 40s)

A to C: Contrast-enhanced CT, late phase: Wall thickening and contrast enhancement are seen in the aortic arch, the aortic arch branches, and the junction of the thoracoabdominal aorta. Although contrast enhancement is seen in the outer part of the thickened wall, contrast enhancement of the inner part is weak and shows double-ring-shaped enhancement (double ring-like sign).

Beginning in April 2018, ^{18}F -FDG PET and PET/CT testing became available at some PET facilities under national health insurance coverage for patients with large-vessel vasculitis in which lesion localization or activity could not be determined with other tests. Because ^{18}F -FDG accumulates in areas of active inflammation, its accumulation in great vessels is a useful finding for diagnosing Takayasu arteritis.¹⁰⁾ In addition, the level of ^{18}F -FDG accumulation is correlated with the clinical activity level of Takayasu arteritis.¹⁰⁾

3. Usefulness of CT and MRI in the chronic phase

Common vascular diseases in the chronic phase are stenosis resulting from reactive intimal thickening and occlusive disease. However, dilated lesions and arterial aneurysms develop when there is severe

vascular smooth muscle cell necrosis or destruction of the elastic fiber layer and mild scarring. Stenotic lesions are commonly seen in vessels such as the left subclavian artery, left common carotid artery, descending thoracic aorta, and abdominal aorta. Collateral circulation develops as a result of stenotic lesions.^{5, 6)} Dilated lesions are commonly seen in the ascending aorta, aortic arch, and brachiocephalic artery. Dilation, stenosis, and occlusive lesions of the aorta and its branches can be visualized well by CTA and MRA and are now rarely evaluated by DSA.^{3, 11-13)} Sensitivity and specificity of 100% and 100%, respectively, for MRA and 95% and 100% for CT have been reported when DSA is used as the gold standard.^{5, 13)} It has also been reported that CTA and MRA can be used to evaluate pulmonary artery stenosis and occlusion, suggesting that they can be used instead of pulmonary blood flow scintigraphy.¹⁴⁾



Figure 2. Takayasu arteritis (acute phase: woman in her 20s)

¹⁸F-FDG PET/CT fusion image: Accumulation is seen in the walls of the thoracic aorta, its branches, and the pulmonary artery. The findings are suggestive of active inflammation.



Figure 3. Takayasu arteritis (chronic phase: woman in her 50s)

Contrast-enhanced CT, MIP image: Striking calcification is seen in the aortic arch. Occlusion of the aortic branches and marked collateral development are seen.

Conditions that define the prognosis of Takayasu arteritis include the following: ① hypertension resulting from the renal artery coarctation or atypical aortic coarctation; ② congestive heart failure resulting from aortic valve insufficiency; ③ ischemic heart disease resulting from coronary artery lesions; and ④ aneurysm rupture. When a complication involving the aorta is present, the 15-year survival rate decreases to 66%. Consequently, to improve the life expectancy of patients, appropriate medical treatment of these conditions must be administered from an early stage, and appropriate surgical treatment is required for patients with severe disease. Recently, CT has also been found to be useful for evaluating coronary artery disease in Takayasu arteritis.^{15, 16)}

Search keywords and secondary sources used as references

PubMed was searched using the following keywords: Takayasu arteritis, CT, and MRI.

In addition, the following were referenced as secondary sources.

- 1) Joint Working Group on Guidelines for the Diagnosis and Treatment of Cardiovascular Disease, Ed.: 2017 Guidelines for Management of Vasculitis Syndrome. Japanese Circulation Society, 2017.
- 2) Hiratzka LF et al: ACCF/AHA/AATS/ACR/ASA/SCA/SCAI/SIR/STS/SVM guidelines for the diagnosis and management of patients with thoracic aortic disease: executive summary. *J Am Coll Cardiol* 55: 1509-1544, 2010

References

- 1) Yamato M et al: Takayasu arteritis: radiographic end angiographic findings in 59 patients. *Radiology* 161 (2): 329-334, 1986
- 2) Park JH: Conventional and CT angiographic diagnosis of Takayasu arteritis. *Int J Cardiol* 54 (suppl): S165-S171, 1996
- 3) Park JH et al: Takayasu arteritis evaluation of mural changes in the aorta and pulmonary artery with CT angiography. *Radiology* 196: 89-93, 1995
- 4) Shama S et al: Morphologic mural changes in the aorta revealed by CT in patients with nonspecific aortoarteritis (Takayasu arteritis). *AJR Am J Roentgenol* 167: 1321-1325, 1996
- 5) Yamada I et al: Takayasu arteritis evaluation of the thoracic aorta with CT angiography. *Radiology* 209: 103-109, 1998
- 6) Matsunaga N et al: Takayasu arteritis protean radiologic manifestations and diagnosis. *Radiographics* 17: 579-597, 1997
- 7) Tso E et al: Takayasu arteritis utility and limitation of magnetic resonance imaging in diagnosis and treatment. *Arthritis Rheum* 46: 1634-1612, 2002
- 8) Choe YH et al: Takayasu's arteritis assessment of disease activity with contrast-enhanced MR imaging. *AJR Am J Roentgenol* 175: 505-51, 2002
- 9) Yamada I et al: Takayasu arteritis evaluation with MR imaging. *Radiology* 188: 89-94, 1993
- 10) Soussan M et al: Management of large-vessel vasculitis with FDG-PET: a systematic literature review and metaanalysis. *Medicine (Baltimore)* 94: e622, 2015
- 11) Kumar S et al: Takayasu's arteritis evaluation with three-dimensional time-of-flight MR angiography. *Eur Radiol* 7: 44-50, 1997
- 12) Natri MV et al: Gadolinium-enhanced three-dimensional MR angiography of Takayasu arteritis. *Radiographics* 24: 773-778, 2004
- 13) Yamada I et al: Takayasu arteritis diagnosis with breath-hold contrast-enhanced three-dimensional MR angiography. *J Magn Reson Imaging* 11: 481-487, 2000
- 14) Sueyoshi E et al: Diagnosis of perfusion abnormality of the pulmonary artery in Takayasu's arteritis using contrast-enhance MR perfusion imaging. *Eur Radiol* 16: 1551-1556, 2006
- 15) Soto ME et al: Coronary OCT angiography of Takayasu arteritis. *J Am Coll Cardiol* 4: 1531-1540, 2011
- 16) Kang EJ et al: Takayasu arteritis assessment of coronary arterial abnormalities with 128 section dual-source CT angiography of the coronary arteries and aorta. *Radiology* 270: 74-81, 2014

BQ 34 Are CT and MRI recommended to determine whether TAVI/TAVR is anatomically indicated for aortic stenosis?

Statement

There is evidence that CT is useful for determining whether TAVI/TAVR is anatomically indicated, and it is therefore recommended. The usefulness of MRI has not yet been established.

Background

Aortic stenosis is a condition in which narrowing of the aortic valve obstructs blood flow from the left ventricle to the ascending aorta. The presence of stenosis is suggested when peak velocity through the aortic valve is > 2 m/s, and severe disease is defined as a peak velocity of > 4 m/s and an aortic valve area of < 1.0 cm² (secondary source 1). The rate of aortic stenosis morbidity is high in elderly individuals. A meta-analysis of studies conducted in Europe and the United States ($n = 9,723$) estimated the prevalence of aortic stenosis to be 12.4% and the prevalence of severe aortic stenosis to be 3.4% in the general population of individuals aged ≥ 75 years.¹⁾

Transcatheter aortic valve implantation (TAVI) and transcatheter aortic valve replacement (TAVR) are treatments first performed in France in 2002.²⁾ Since then, they have been accepted as alternatives to surgical aortic valve replacement in patients for whom surgery is contraindicated and those at high surgical risk, and they have become progressively more widely implemented in recent years.³⁻⁵⁾ A 2013 meta-analysis estimated that TAVI/TAVR was indicated for approximately 290,000 patients in Europe and the United States (approximately 190,000 in the Europe and 100,000 in North America), and that it was newly indicated for approximately 27,000 patients annually (approximately 18,000 annually in Europe and 9,000 annually in North America).¹⁾ As of March 2020, the main devices used in Japan are the balloon-expandable SAPIEN 3 bioprosthetic valve (Edwards Lifesciences) and the self-expanding Evolut™ PRO system (Medtronic; Fig. 1). A transfemoral approach is generally selected (Fig. 2A). However, if this route is not feasible because of the patient's background, a transapical (Fig. 2B), transsubclavian, or transaortic (Fig. 2C) approach is selected.

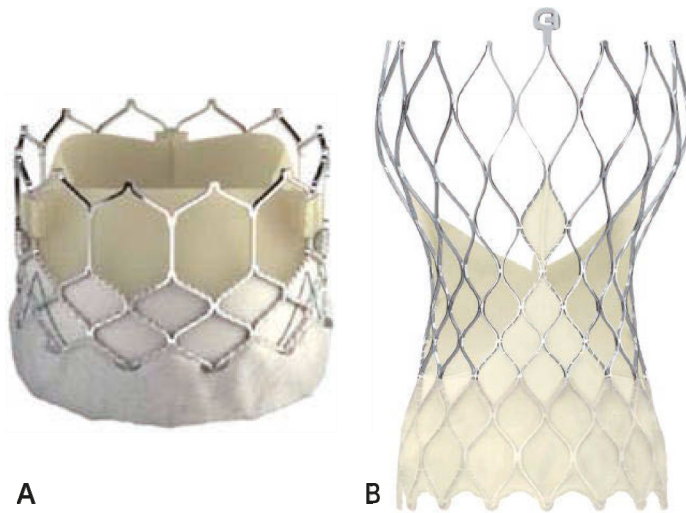


Figure 1. Prosthetic valves used in TAVI/TAVR

A: Balloon-expandable SAPIEN 3 (provided by Edwards Lifesciences)

B: Self-expanding Evolut™ PRO (provided by Medtronic Japan)

Explanation

To select the appropriate bioprosthetic valve size for TAVI/TAVR, the aortic valve annulus must be accurately measured. If the bioprosthetic valve is too large for the annulus, rupture may occur, and this is often fatal.⁴⁾ Conversely, bioprosthetic valves that are too small for the annulus have been found to increase the frequency of perivalvular aortic regurgitation and adversely affect outcomes.⁶⁻⁸⁾ In the evaluation performed before TAVI/TAVR, the diameter of the aortic valve annulus has historically been measured by performing aortography, transthoracic echocardiography, or transesophageal echocardiography. However, measurements are often discrepant.^{9, 10)} The reason these 2-dimensional tests have major limitations is that the aortic valve annulus is elliptical rather than circular.^{9, 10)} With 2D echocardiography, the diameter is generally measured near the short-axis diameter of the elliptical annulus. Consequently, the diameter measured with 3D CT is greater than that obtained with echocardiography. The use of CT measurement to select valve size has been reported to reduce post-TAVI/TAVR aortic valve regurgitation, as compared with size selection based on echocardiography.¹¹⁾ CT is currently the gold standard for measuring the diameter of the aortic valve annulus.⁵⁾

Moreover, in pre-TAVI/TAVR examinations, CT provides useful information about access routes, including the apex and vasculature from the aortic root to the bilateral common femoral artery. Together with the patient background characteristics, this information plays an important role in selecting a transfemoral (Fig. 2A), transapical (Fig. 2B), or other approach.^{4, 5)} Furthermore, the projection image orthogonal to the aortic valve, i.e., the perpendicular view during TAVI/TAVR procedure/contrast imaging (Fig. 3), can be estimated from pre-TAVI/TAVR CT images,^{4, 5)} enabling the contrast medium dose to be reduced during the TAVI/TAVR procedure.

Based on the above considerations, CT is recommended to determine whether TAVI/TAVR is anatomically indicated in patients with aortic stenosis.^{4, 5)}

The usefulness of MRI for determining whether TAVI/TAVR is anatomically indicated has not yet been established.

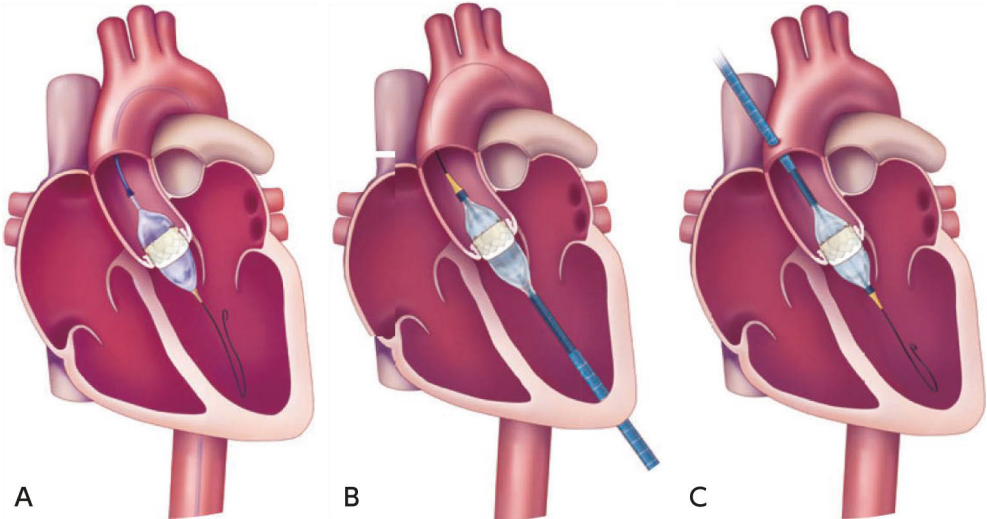


Figure 2. Various approaches for TAVI/TAVR
A: Transfemoral approach, B: Transapical approach, C: Transaortic approach
(provided by Edwards Lifesciences)

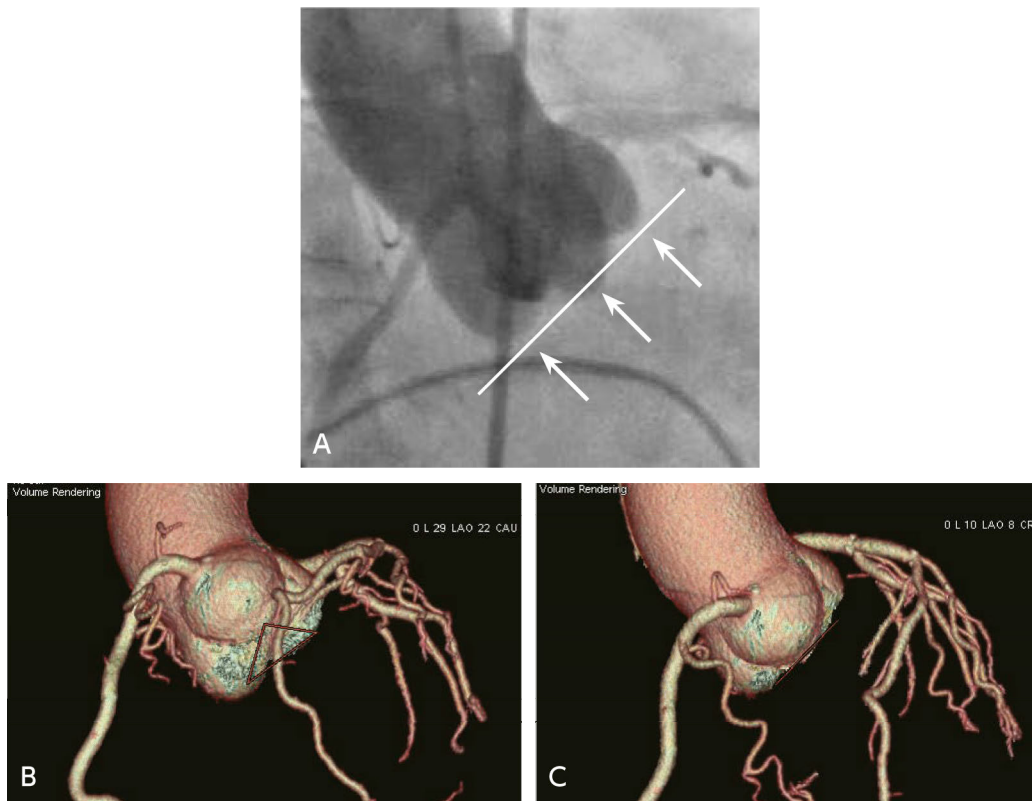


Figure 3. Pre-TAVI/TAVR CT estimate on the perpendicular view during TAVI/TAVR procedure/contrast imaging.

Search keywords and secondary sources used as references

PubMed was searched using the following keywords: aortic stenosis, transcatheter aortic valve implantation, and transcatheter aortic valve replacement.

In addition, the following was referenced as a secondary source.

- 1) Nishimura RA et al: 2014 AHA/ACC guideline for the management of patients with valvular heart disease: a report of the American College of Cardiology/American Heart Association Task Force on Practice Guidelines. *Circulation* 129 (23):

References

- 1) Osnabrugge RL et al: Aortic stenosis in the elderly: disease prevalence and number of candidates for transcatheter aortic valve replacement: a meta-analysis and modeling study. *J Am Coll Cardiol* 62 (11): 1002-1012, 2013
- 2) Cribier A et al: Percutaneous transcatheter implantation of an aortic valve prosthesis for calcific aortic stenosis: first human case description. *Circulation* 106 (24): 3006-3008, 2002
- 3) Holmes DR et al: 2012 ACCF/AATS/SCAI/STS expert consensus document on transcatheter aortic valve replacement. *J Am Coll Cardiol* 59 (13): 1200-1254, 2012
- 4) Achenbach S et al: SCCT expert consensus document on computed tomography imaging before transcatheter aortic valve implantation (TAVI)/transcatheter aortic valve replacement (TAVR). *J Cardiovasc Comput Tomogr* 6 (6): 366-380, 2012
- 5) Blanke P et al: Computed tomography imaging in the context of transcatheter aortic valve implantation (TAVI)/transcatheter aortic valve replacement (TAVR): an expert consensus document of The Society of Cardiovascular Computed Tomography. *JACC Cardiovasc Imaging* 12 (1): 1-24, 2019
- 6) Gilard M et al: Registry of transcatheter aortic-valve implantation in high-risk patients. *N Engl J Med* 366 (18): 1705-1715, 2012
- 7) Sinning JM et al: Aortic regurgitation index defines severity of peri-prosthetic regurgitation and predicts outcome in patients after transcatheter aortic valve implantation. *J Am Coll Cardiol* 59 (13): 1134-1141, 2012

- 8) Kodali SK et al: Two-year outcomes after transcatheter or surgical aortic-valve replacement. *N Engl J Med* 366 (18): 1686-1695, 2012
- 9) Altiok E et al: Comparison of two-dimensional and three-dimensional imaging techniques for measurement of aortic annulus diameters before transcatheter aortic valve implantation. *Heart (British Cardiac Society)* 97 (19): 1578-1584, 2011
- 10) Ng AC et al: Comparison of aortic root dimensions and geometries before and after transcatheter aortic valve implantation by 2-and 3-dimensional transesophageal echocardiography and multislice computed tomography. *Circulation Cardiovascular imaging* 3 (1): 94-102, 2010
- 11) Jilaihawi H et al: Cross-sectional computed tomographic assessment improves accuracy of aortic annular sizing for transcatheter aortic valve replacement and reduces the incidence of paravalvular aortic regurgitation. *J Am Coll Cardiol* 59 (14): 1275-1286, 2012

FQ 3 Is preoperative identification of the artery of Adamkiewicz recommended before open repair or endovascular repair of a thoracic aortic aneurysm or thoracoabdominal aortic aneurysm?

Statement

There is a tendency to recommend identification of the artery of Adamkiewicz as a preoperative examination, although the evidence is not sufficient in the case of open repair.

Although the evidence is also insufficient in the case of endovascular repair, identification of the artery can be considered in cases if the critical zone is to be covered or in patients whose aortic pathologies require extensive coverage.

Background

One of the most serious complications in patients undergoing thoracic descending aortic aneurysm and thoracoabdominal aortic aneurysm repair is spinal cord ischemia. Preoperative identification of the artery of Adamkiewicz using CT or MRI can help prevent postoperative spinal cord injury.

Explanation

In the thoracolumbar spinal cord, the feeding artery of the anterior spinal artery is the great anterior radiculomedullary artery, also known as the artery of Adamkiewicz, with a diameter of approximately 1 mm. This artery supplies the lower one-third of the spinal cord, commonly originating between the 8th intercostal artery and the 1st lumbar artery.¹⁾

The distal portion of the artery of Adamkiewicz and the anterior spinal artery form a “hairpin turn” configuration. This characteristic morphology is an important landmark when identifying the artery of Adamkiewicz on CT or MRI. Although invasive angiography was previously performed for identification of the artery of Adamkiewicz,²⁾ CT and MRI are now usually used. In a meta-analysis, the visualization rates of CT and MRI were found to be 88.1% and 88.3%, respectively.³⁾ On the other hand, there are still few studies examining whether preoperative identification of the artery of Adamkiewicz prevents postoperative spinal cord ischemia. We will discuss open repair and endovascular repair separately.

In the case of open repair, a multicenter, retrospective cohort study of more than 2,000 patients in Japan (JASPAR study) has been reported.

The results showed that, in open repair for aortic segments involving the origin of the artery of Adamkiewicz, having no reconstruction of the artery of Adamkiewicz was a significant risk factor for postoperative spinal cord ischemia (odds ratio 2.79, 95% CI, 1.14 to 6.79, $p = 0.024$).⁴⁾ There have been several reports from single centers. Hyodoh et al. found a significant difference ($p < 0.01$) in the incidence

of postoperative spinal cord ischemia in 50 patients in the group operated with identification of the artery of Adamkiewicz and in the group operated without identification ($p < 0.01$).⁵⁾

Preoperative identification of the artery of Adamkiewicz in combination with other spinal cord protection methods has also been reported. Tanaka et al. reported the usefulness of selective reconstruction of the identified intercostal artery from which the artery of Adamkiewicz originated and hypothermia.⁶⁾ Similarly, Furukawa et al. showed that selective perfusion and reconstruction of identified segmental arteries were useful.⁷⁾ In addition, Ogino et al. and Nijenhuis et al. reported that preoperative identification of the artery of Adamkiewicz in combination with motor-evoked potentials was useful.^{8,9)}

As described above, although the evidence is not sufficient, identification of the artery of Adamkiewicz tends to be recommended as a preoperative examination for open repair. (secondary source 1).

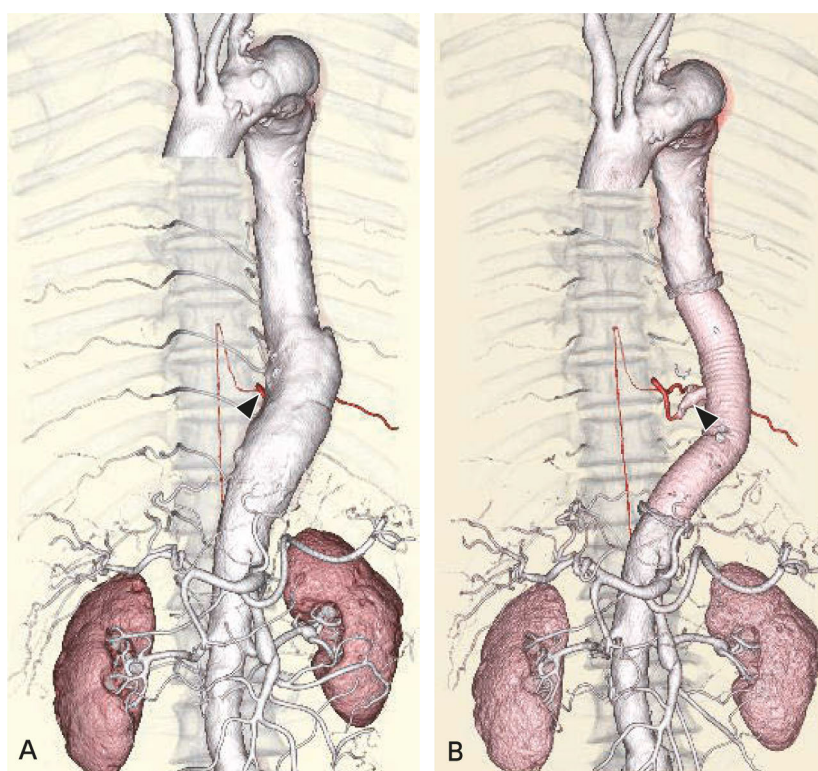


Figure. Preoperative identification of the artery of Adamkiewicz

A: Preoperative contrast-enhanced CT, VR image; B: Postoperative contrast-enhanced CT, VR image

The patient was a man in his 60s. DeBakey type IIIb dissecting aortic aneurysm. Preoperative CT shows the artery of Adamkiewicz originating from the left 10th intercostal artery (A►). The prosthetic graft replacement of the descending aorta and reconstruction of the left 10th intercostal artery (B►) were performed. Spinal cord ischemia did not occur postoperatively.

The incidence of spinal cord ischemia is lower with endovascular repair than with open repair. Moreover, the above-mentioned JASPAR study did not prove the usefulness of preoperative identification of the artery of Adamkiewicz in the case of endovascular repair.⁴⁾ On the other hand, some studies have reported the usefulness of preoperative identification. Kamada et al. reported a single-center, retrospective study of 74

cases that showed that no spinal cord ischemia occurred in the group treated with preoperative identification of the artery of Adamkiewicz, but it did occur in 23.8% of those in a group for which the artery of Adamkiewicz was not identified preoperatively.¹⁰⁾ Matsuda et al. also reported that preoperative identification of the artery of Adamkiewicz was useful in determining the landing zones for stent grafts.¹¹⁾ Furthermore, it has been shown that occlusion of the artery of Adamkiewicz by a stent-graft is a risk factor for spinal cord ischemia in patients whose thoracic aortas require extensive coverage.¹²⁾

As the above findings indicate, although the evidence is insufficient in the case of endovascular repair, identification of the artery of Adamkiewicz can be considered in cases if the critical zone where the artery of Adamkiewicz frequently originates is to be covered or the repair length is long.

Although either CT or MRI can be selected for the examination, CT is generally easier to perform. Usually, CT is the first choice, and MRI is recommended for use in cases in which CT was not satisfactory for identification.¹³⁾ However, visualization of the artery of Adamkiewicz may be affected by the performance of the CT or MRI system. So, it is important to understand the characteristics of the equipment used at each institution before selecting an examination method.

Search keywords and secondary sources used as references

PubMed was searched using the following keywords: aortic aneurysm, Adamkiewicz, surgery or repair, TEVAR, complication, and spinal cord ischemia. The period searched was from January 1, 2009 to June 30, 2019; hits were obtained for 70 articles. Articles obtained by a hand search were also used.

In addition, the following was referenced as a secondary source.

- 1) Ogino H, et al.: 2020 Guideline on Diagnosis and Treatment of Aortic Aneurysm and Aortic Dissection. Japanese Circulation Society, 2020.

References

- 1) Koshino T et al: Does the Adamkiewicz artery originate from the larger segmental arteries? *J Thorac Cardiovasc Surg* 117 (5): 898-905, 1999
- 2) Kieffer E et al: Spinal cord arteriography: a safe adjunct before descending thoracic or thoracoabdominal aortic aneurysmectomy. *J Vasc Surg* 35 (2): 262-268, 2002
- 3) Tattera D et al: Artery of Adamkiewicz: a meta-analysis of anatomical characteristics. *Neuroradiology* 61 (8): 869-880, 2019
- 4) Tanaka H et al: The impact of preoperative identification of the Adamkiewicz artery on descending and thoracoabdominal aortic repair. *J Thorac Cardiovasc Surg* 151 (1): 122-128, 2016
- 5) Hyodoh H et al: Usefulness of preoperative detection of artery of Adamkiewicz with dynamic contrast-enhanced MR angiography. *Radiology* 236 (3): 1004-1009, 2005
- 6) Tanaka H et al: Recent thoraco-abdominal aortic repair outcomes using moderate-to-deep hypothermia combined with targeted reconstruction of the Adamkiewicz artery†. *Interact Cardiovasc Thorac Surg* 20 (5): 605-610, 2015
- 7) Furukawa K et al: Operative strategy for descending and thoracoabdominal aneurysm repair with preoperative demonstration of the Adamkiewicz artery. *Ann Thorac Surg* 90 (6): 1840-1846, 2010
- 8) Ogino H et al: Combined use of Adamkiewicz artery demonstration and motor-evoked potentials in descending and thoracoabdominal repair. *Ann Thorac Surg* 82 (2): 592-596, 2006
- 9) Nijenhuis RJ et al: Magnetic resonance angiography and neuromonitoring to assess spinal cord blood supply in thoracic and thoracoabdominal aortic aneurysm surgery. *J Vasc Surg* 45 (1): 71-77, 2007
- 10) Kamada T et al: Strategy for thoracic endovascular aortic repair based on collateral circulation to the artery of Adamkiewicz. *Surg Today* 46 (9): 1024-1030, 2016

- 11) Matsuda H et al: Multidisciplinary approach to prevent spinal cord ischemia after thoracic endovascular aneurysm repair for distal descending aorta. *Ann Thorac Surg* 90 (2): 561-565, 2010
- 12) Matsuda H et al: Spinal cord injury is not negligible after TEVAR for lower descending aorta. *Eur J Vasc Endovasc Surg* 39 (2): 179-186, 2010
- 13) Takagi H et al: Identifying the Adamkiewicz artery using 3-T time-resolved magnetic resonance angiography: its role in addition to multidetector computed tomography angiography. *Jpn J Radiol* 33 (12): 749-756, 2015

BQ 35 Is nuclear medicine testing recommended for diagnosis and elucidation of pathology in patients with chronic heart failure?

Statement

Nuclear medicine testing has been shown to be highly accurate in noninvasively differentiating between chronic heart failure etiologies, and there is sufficient evidence to support its use in determining treatment. Moreover, there is abundant evidence of its usefulness in risk stratification and prognosis prediction, and it is therefore recommended for these purposes.

Background

Although ischemic heart disease is considered the typical disease in which chronic heart failure is manifested, other causes of heart failure include heart valve disease, cardiomyopathy, hypertensive heart disease, and congenital heart disease. The usefulness of echocardiography diagnosis of morphological abnormalities has long been established. However, differentiating ischemic heart failure from non-ischemic heart failure is occasionally difficult. Although coronary angiography is useful for diagnosing ischemic heart disease, it is invasive. A non-invasive method of diagnosis is needed.

The left ventricular ejection fraction (LVEF), end-diastolic volume (EDV), and end-systolic volume (ESV) are used to assess the severity of chronic heart failure and predict prognosis. However, their accuracy as prognostic factors is low, at least in the case of cardiomyopathy. In recent years, signs such as the presence of decreased right ventricular function and pulmonary hypertension and cardiac sympathetic abnormalities have drawn attention as factors for predicting prognosis.

The first half of this section describes nuclear medicine testing for pathology differentiation. The second half describes nuclear medicine testing for prognostic assessment.

Explanation

1. Pathology differentiation

Heart failure has a variety of causes, and treatment strategies vary greatly depending on whether it is ischemic heart failure or another type, making differentiation important. Stress perfusion SPECT is useful for diagnosing ischemia. In a study of 164 patients with chronic heart failure, Danias et al., using the total defect score with stress, reported sensitivity and specificity of 87% and 63%, respectively, for this modality.¹⁾

In Japan, ¹²³I-beta-methyl-p-iodophenyl-pentadecanoic acid (BMIPP) myocardial scintigraphy is widely used as a method that does not involve stress, and its use in diagnosing both ischemic and non-ischemic disease has been investigated.^{2, 3)} In recent years, the mismatch score for dual-isotope scintigraphy with BMIPP and ²⁰¹Tl (TL) accumulation has been used to differentiate between ischemic cardiomyopathy and dilated cardiomyopathy (Fig. 1). In an examination of 501 consecutive patients, Abe et al. reported

sensitivity and specificity of 84% and 83%, respectively, with this method. Thus, there appears to be sufficient evidence to support the use of this approach in actual clinical practice.³⁾

In recent years, cardiac amyloidosis has attracted attention as a cause of heart failure in elderly individuals, particularly heart failure with preserved left ventricular ejection fraction (HFpEF). Recent studies have shown that cardiac amyloidosis is not a rare disorder. The amyloids that are related to heart disease are mainly AL amyloid, which is derived from the immunoglobulin light chain, and ATTR amyloid, which is caused by a transthyretin abnormality. The prognosis varies greatly with these 2 amyloids. The diagnostic agent ^{99m}Tc-pyrophosphate (PYP), which is used to diagnose acute myocardial infarction, has been found to accumulate in ATTR amyloid specifically (Fig. 2),⁴⁾ and it is becoming a standard method of diagnosis in other countries. In a study of 171 patients at 3 centers, examination of its diagnostic accuracy showed sensitivity and specificity of 91% and 92%, respectively.⁵⁾

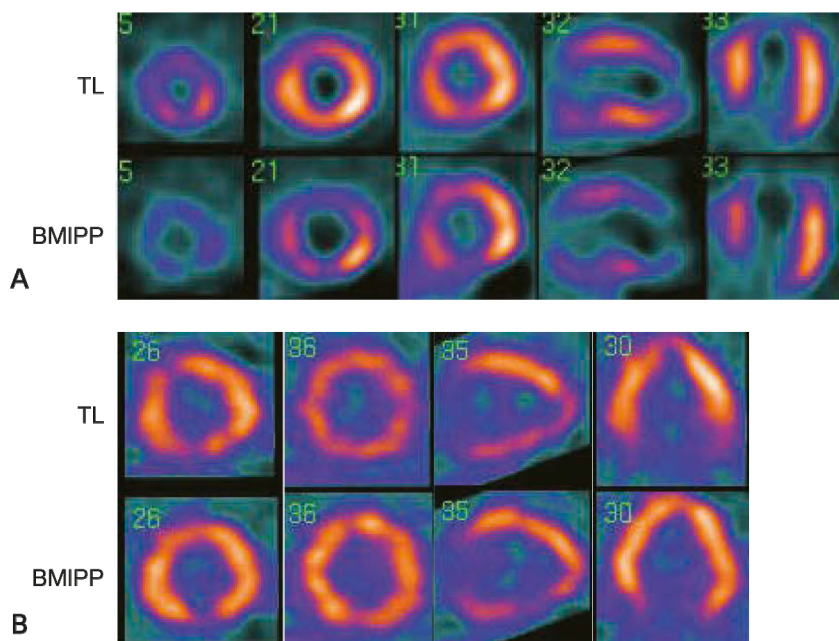


Figure 1. Simultaneous dual-isotope SPECT with TL and BMIPP, short axis, long axis image

A: Ischemic cardiomyopathy, B: Dilated cardiomyopathy

In A, a severe BMIPP defect is present from the anterior wall to the apex and inferoposterior wall. The defect is more severe than with TL. The patient's LVEF was 27%, and 3-vessel disease was seen by coronary angiography. In B, no apparent accumulation defect is seen with either tracer. These are typical findings for dilated cardiomyopathy.

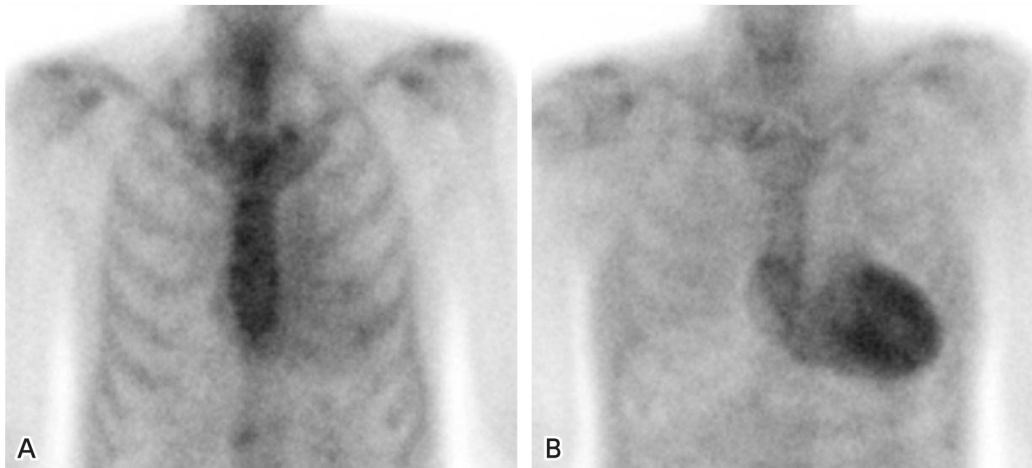


Figure 2. PYP scintigraphy in patients with heart failure and marked left ventricular hypertrophy, frontal view, planar image

A: Patient amyloid-negative on myocardial biopsy, B: Patient with ATTR cardiac amyloidosis

Clear myocardial accumulation is seen in the patient with ATTR cardiac amyloidosis. The heart to contralateral lung ratio (H/CL ratio) is 1.40 for the amyloid-negative patient and 2.02 for the patient with ATTR cardiac amyloidosis.

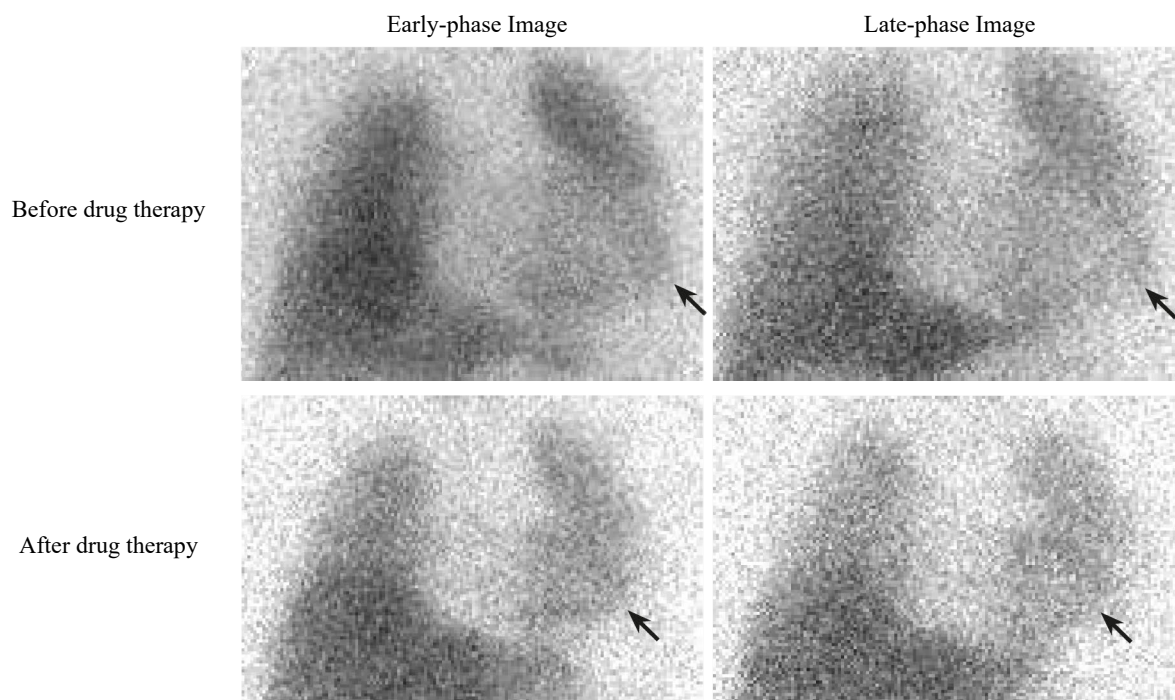


Figure 3. MIBG myocardium scintigraphy in a patient with dilated cardiomyopathy, frontal view, planar image

In the top row, the heart-to-mediastinum uptake ratio (H/M ratio) is low (1.53) in the late-phase image acquired before drug therapy. The patient was judged to have severe heart failure. After 6 months of drug therapy with a beta-blocker and ACE inhibitor, the left ventricle has decreased in size, and the H/M ratio has improved to 2.20 (→).

2. Prognostic assessment

As a compensatory mechanism for the decreased pumping function of the heart in chronic heart failure, the sympathetic nervous system and humoral factors are activated. However, their excessive activation can trigger catecholamine-induced myocardial damage and fatal arrhythmias. Monitoring of sympathetic function is therefore considered an effective means of assessing the relationship to myocardial damage and treatment efficacy. ^{123}I -MIBG (MIBG) is a catecholamine analog that enables imaging of catecholamine kinetics in sympathetic nerve endings. Early-phase imaging is normally performed 15 minutes after its intravenous injection, and late-phase imaging is performed 4 hours after intravenous injection. The H/M uptake ratio and washout rate (WR) at 4 hours are then calculated. Numerous studies have found that the lower the late-phase H/M ratio and the higher the WR, the poorer the prognosis (Fig. 2). A meta-analysis of 2-year⁶⁾ and 5-year⁷⁾ outcomes in the multicenter ADMIRE study conducted in Europe and the United States and reports from 6 facilities in Japan⁸⁾ showed that the MIBG late-phase H/M ratio reflected prognosis with high accuracy. Moreover, an examination of 116 patients for whom an implantable cardioverter defibrillator (ICD) was indicated found that, when the extent of the defect seen on MIBG late-phase SPECT images was large, the rates of appropriate ICD therapy and cardiac death increased significantly.⁹⁾ However, it should be noted that technical standardization is essential for H/M measurement.¹⁰⁾

Although small in number, studies have also found BMIPP to be useful for prognosis prediction. Zavadovsky et al. found BMIPP to be better than perfusion scintigraphy for predicting response to cardiac resynchronization therapy in dilated cardiomyopathy.¹¹⁾ In an examination of 804 patients with HFpEF without ischemia, Hashimoto et al. found the BMIPP defect score to be useful for prognosis stratification. With regard to cardiac amyloidosis prognosis prediction using PYP, it has been reported that prognosis stratification can be performed using a heart-to-contralateral lung ratio (H/CL ratio) of 1.6 as the cutoff¹²⁾ (Fig. 3).

Search keywords and secondary sources used as references

PubMed was searched using the following keywords: BMIPP, MIBG, PYP, heart failure, prognosis, cardiomyopathy, cardiac amyloidosis, and prognosis.

In addition, the following were referenced as secondary sources.

- 1) Japanese Circulation Society, Ed.: 2010 Guidelines for Clinical Use of Cardiac Nuclear Medicine (JCS 2010). Japanese Circulation Society, 2010.
- 2) Dorbala S et al: ASNC/AHA/ASE/EANM/HFSA/ISA/SCMR/SNMMI expert consensus recommendations for multimodality imaging in cardiac amyloidosis: Part 1 of 2-evidence base and standardized methods of imaging. *J Nucl Cardiol* 26: 2065-2123. 2019
- 3) Bokhari S et al: Standardization of $^{99\text{m}}\text{Tc}$ pyrophosphate imaging methodology to diagnose TTR cardiac amyloidosis. *J Nucl Cardiol* 25: 181-190, 2018

References

- 1) Danias PG et al: Usefulness of electrocardiographic-gated stress technetium-99 m sestamibi single-photon emission computed tomography to differentiate ischemic from nonischemic cardiomyopathy. *Am J Cardiol* 94: 14-19, 2004
- 2) Ishida Y et al: Myocardial imaging with 123I-BMIPP in patients with congestive heart failure. *Int J Card Imaging* 15: 71-77, 1999
- 3) Abe H et al: Non-invasive diagnosis of coronary artery disease by ¹²³I-BMIPP/²⁰¹TlCl dual myocardial SPECT in patients with heart failure. *Int J Cardiol* 176: 969-974, 2014
- 4) Bokhari S et al: ^{99m}Tc-pyrophosphate scintigraphy for differentiating light-chain cardiac amyloidosis from the transthyretin-related familial and senile cardiac amyloidoses. *Circ Cardiovasc Imaging* 6: 195-201, 2013
- 5) Castano A et al: multicenter study of planar technetium 99 m pyrophosphate cardiac imaging: predicting survival for patients with ATTR cardiac amyloidosis. *JAMA Cardiol* 1: 880-889, 2016
- 6) Jacobson AF et al: Myocardial iodine-123 meta-iodobenzylguanidine imaging and cardiac events in heart failure. Results of the prospective ADMIRE-HF (AdreView Myocardial Imaging for Risk Evaluation in Heart Failure) study. *J Am Coll Cardiol* 55: 2212-2221, 2010
- 7) Agostini D et al: Prognostic usefulness of planar ¹²³I-MIBG scintigraphic images of myocardial sympathetic innervation in congestive heart failure: follow-up data from ADMIRE-HF. *J Nucl Cardiol*, 2019
- 8) Nakata T et al: A pooled analysis of multicenter cohort studies of ¹²³I-mIBG imaging of sympathetic innervation for assessment of long-term prognosis in heart failure. *JACC Cardiovasc Imaging* 6: 772-784, 2013
- 9) Boogers MJ et al: Cardiac sympathetic denervation assessed with 123-iodine metaiodobenzylguanidine imaging predicts ventricular arrhythmias in implantable cardioverter-defibrillator patients. *J Am Coll Cardiol* 55: 2769-2777, 2010
- 10) Nakajima K et al: Normal values and standardization of parameters in nuclear cardiology: Japanese Society of Nuclear Medicine working group database. *Ann Nucl Med* 30: 188-199, 2016
- 11) Zavadovsky KV et al: Perfusion and metabolic scintigraphy with ¹²³I-BMIPP in prognosis of cardiac resynchronization therapy in patients with dilated cardiomyopathy. *Ann Nucl Med* 30: 325-333, 2016
- 12) Hashimoto H et al: Prognostic value of 123I-BMIPP SPECT in patients with nonischemic heart failure with preserved ejection fraction. *J Nucl Med* 59: 259-265, 2018